Cell-to-cell heterogeneity of phosphate gene expression in yeast is controlled by alternative transcription, 14-3-3 and Spl2

Crooijmans, M.E.; Delzenne, T.O.; Hensen, T.; Darehei, M.; Winde, J.H. de; Heusden, G.P.H. van

BBA - Gene Regulatory Mechanisms 1864 (2021) 194714

Contents lists available at ScienceDirect

BBA - Gene Regulatory Mechanisms

journal homepage: www.elsevier.com/locate/bbagrm

Cell-to-cell heterogeneity of phosphate gene expression in yeast is controlled by alternative transcription, 14-3-3 and Spl2

Marjolein E. Crooijmans, Tijn O. Delzenne, Tim Hensen, Mina Darehei, Johannes H. de Winde, G. Paul H. van Heusden *

Institute of Biology, Leiden University, Leiden, the Netherlands

ARTICLE INFO

Keywords:
Phosphate metabolism
Saccharomyces cerevisiae
Non-coding transcription
Bimodal gene expression
Transcription start site

ABSTRACT

Dependent on phosphate availability the yeast *Saccharomyces cerevisiae* expresses either low or high affinity phosphate transporters. In the presence of phosphate yeast cells still express low levels of the high affinity phosphate transporter Pho84. The regulator Spl2 is expressed in approximately 90% of the cells, and is not expressed in the remaining cells. Here we report that deletion of *RRP6*, encoding an exonuclease degrading non-coding RNA, or *BMH1*, encoding the major 14-3-3 isoform, resulted in less cells expressing *SPL2* and in increased levels of RNA transcribed from sequences upstream of the *SPL2* coding region. *SPL2* stimulates its own expression and that of *PHO84* ensuing a positive feedback. Upon deletion of the region responsible for upstream *SPL2* transcription almost all cells express *SPL2*. These results indicate that the cell-to-cell variation in *PHO84* and *SPL2* expression is dependent on a specific part of the *SPL2* promoter and is controlled by Bmh1 and Spl2.

1. Introduction

For microorganisms nutrient uptake is essential for survival and these organisms have to be able to adapt rapidly to changes in availability of the various nutrients; for review see: [1–3]. For many nutrients microorganisms have the ability to express either high or low affinity transporters allowing nutrient uptake when concentrations in the environment are low or high, respectively [2]. This has been clearly demonstrated for phosphate uptake by the yeast *Saccharomyces cerevisiae*. This organism can express low and high affinity phosphate transporters depending on phosphate availability.

In *S. cerevisiae* phosphate homeostasis is a tightly regulated process; for review see [4–7]. When phosphate is abundant the low affinity transporters Pho87 and Pho90 are responsible for phosphate uptake [4,8]. Upon phosphate starvation intracellular phosphate levels decrease resulting in inactivation of the Pho80–Pho85 complex. As a consequence, the Pho4 transcription factor becomes de-phosphorylated and enters the nucleus resulting in expression of more than 20 genes involved in phosphate uptake (PHO genes) [9,10]. These genes include among others *PHO5* [11], encoding an extracellular phosphatase, *PHO84*, encoding a high affinity phosphate transporter [12] and *SPL2*, encoding a protein with some similarity to cyclin-dependent kinase inhibitors [13]. *SPL2* was shown to be involved in translocation of the low affinity Pho87 transporter from the cell membrane to the vacuole during phosphate starvation [14]. Expression of *PHO84* is further regulated by transcription in the antisense direction [15–17]. When phosphate is available, antisense transcription may result in histone modifications and inaccessibility of the promoter for transcription in the sense direction. In *Schizosaccharomyces pombe* genes related to phosphate uptake are regulated by non-coding RNA as well [18–20].

At intermediate phosphate concentrations individual cells express predominantly either low- or high-affinity transporters [21]. This may provide the population a strategy for anticipating changes in environmental phosphate levels. This heterogeneity in gene expression is stabilized by positive and negative feedback loops in which Spl2p is involved [21]. In our previous study we showed that in the presence of phosphate GFP-tagged *SPL2* is expressed in more than 90% of the cells, and in a small number of cells no expression is seen [22]. On the other hand, upon deletion of *BMH1*, encoding the major 14-3-3 protein isoform [23–25], *SPL2-GFP* is expressed in only 20 to 30% of the cells and the majority of the cells are not expressing *SPL2-GFP*. After 60 min of phosphate or potassium starvation expression of *SPL2-GFP* is strongly induced in all cells, both in the wild type strain and in the bmh1Δ deletion mutant. This indicates involvement of 14-3-3 proteins in the heterogeneity of *PHO* gene expression when phosphate is available.

In this study we further investigated the role of Bmh1 and non-

* Corresponding author.
E-mail address: g.p.h.van.heusden@biology.leidenuniv.nl (G.P.H. van Heusden).

https://doi.org/10.1016/j.bbagrm.2021.194714
Received 11 November 2020; Received in revised form 27 April 2021; Accepted 27 April 2021
Available online 7 May 2021

coding RNA in the regulation of phosphate homeostasis and in the cell-to-cell variation of the expression of *SPL2* and *PHO84*. We mostly focused on conditions in which phosphate was available rather than on conditions of phosphate starvation. To allow comparison of all experimental data we standardized growth conditions, all data were obtained from cultures of exponentially growing cells in liquid YNB medium containing 7.2 mM phosphate (see Materials and methods). Our studies indicate that the expression of the *PHO* genes *PHO84* and *SPL2* and the cell-to-cell variation of *PHO84* and *SPL2* expression is dependent on the transcriptional regulation of *SPL2*. Expression of *PHO84* and *SPL2* is stimulated by *SPL2* showing a positive feedback loop which can stabilize the heterogenic expression of *SPL2*. A new model for the regulation of *SPL2* and *PHO84* is proposed.

2. Materials and methods

2.1. Strains, plasmids, primers, media and culture conditions

In this study the yeast strain BY4741 and strains derived from BY4741 were used, as listed in Table 1. Plasmids and primers used in this study are listed in Tables 2 and 3, respectively. Yeast transformations were performed using the lithium acetate method [26].

For cultivation at defined phosphate concentrations phosphate-free YNB medium (Formedium, UK) was used. If required, histidine, leucine, methionine and/or uracil were added to a final concentration of 20 mg/L, potassium phosphate (pH 5.8) was added to a final concentration of 7.2 mM and potassium chloride was added to a final concentration of 50 mM. To study the effects of phosphate starvation yeast strains were grown overnight at 30 °C in supplemented phosphate-free YNB medium containing 7.2 mM potassium phosphate (pH 5.8) and 50 mM KCl. This culture was used to inoculate two times 50 mL of supplemented YNB medium containing 7.2 mM potassium phosphate (pH 5.8) and 50 mM KCl yielding A_{620nm} 0.1. These cultures were grown to A_{620nm} 0.5 and cells were isolated by centrifugation. Cells from one culture were washed twice with supplemented YNB medium containing 7.2 mM potassium phosphate (pH 5.8) and 50 mM KCl and resuspended in 50 mL supplemented YNB medium. Cells from the other culture were washed twice with supplemented YNB medium lacking phosphate and resuspended in 50 mL supplemented YNB medium lacking phosphate but containing 50 mM KCl. Both cultures were incubated at 180 rpm at 30 °C for 60 min. For transcriptome analysis cultures were frozen immediately in liquid nitrogen.

Table 1
Yeast strains used in this study.

Strain	Genotype	Source/ reference
BY4741	*MATa his3Δ1 leu2Δ0 met15Δ0 ura3Δ0*	Euroscarf
bmh1Δ (GG3240)	*bmh1Δ::loxP* in BY4741	[22]
rrp6Δ	*rrp6Δ::kanMX* in BY4741	Euroscarf
spl2Δ	*spl2Δ::kanMX* in BY4741	Euroscarf
pho4Δ	*pho4Δ::kanMX* in BY4741	Euroscarf
BY4741 SPL2-GFP (GG3434)	*SPL2-GFP (HIS3)* in BY4741	[22]
bmh1Δ SPL2-GFP (GG3435)	*bmh1Δ::loxP SPL2-GFP (HIS3)* in BY4741	[22]
rrp6Δ SPL2-GFP (GG3472)	*rrp6Δ::kanMX SPL2-GFP (HIS3)* in BY4741	This study
pho4Δ SPL2-GFP (GG3473)	*pho4Δ::kanMX SPL2-GFP (HIS3)* in BY4741	This study
BY4741 (P_{PHO84}-GFP) (GG3437)	*leu2Δ0*::pRS305[P_{PHO84}-*GFP*](*LEU2*) in BY4741	[22]
BY SPL2-GFP ΔP (GG3467)	BY4741 *SPL2-GFP(HIS3)* Δbox P	This study
BY P_{PHO84}-GFP ΔP (GG3469)	BY4741 *leu2Δ0*::pRS305[Ppho84-*GFP*](*LEU2*] Δbox P	This study
rrp6 SPL2-GFP ΔP (GG3471)	*rrp6Δ::kanMX* in BY4741 *SPL2-GFP* (*HIS3*) Δbox P	This study
bmh1 SPL2-GFP ΔP (GG3484)	*bmh1Δ::loxP* in BY4741 *SPL2-GFP (HIS3)* ΔboxP	This study
BY4741 ΔP (GG3474)	BY4741 Δbox P	This study
rrp6 ΔP (GG3475)	rrp6Δ Δbox P	This study
BY4741 Tpho84-Tcyc1 (GG3479)	BY4741 *PHO84*(Terminator) Δ::*CYC1* (Terminator)	This study
bmh1 Tpho84-Tcyc1 (GG3480)	bmh1Δ *PHO84*(Terminator) Δ::*CYC1* (Terminator)	This study
rrp6 Tpho84-Tcyc1 (GG3481)	rrp6Δ *PHO84*(Terminator) Δ::*CYC1* (Terminator)	This study
spl2 Tpho84-Tcyc1 (GG3482)	spl2Δ *PHO84*(Terminator) Δ::*CYC1* (Terminator)	This study

Table 2
Plasmids.

Plasmid	Properties	Source/reference
pYM28	Plasmid for tagging with GFP. *HIS* marker.	[27]
pRS316	Yeast centromeric plasmid. *URA3* marker.	[61]
pRS316[RRP6] (pRUL1377)	pRS316 with a 2546 bp genomic DNA fragment with *RRP6*	This study
pRS316[SPL2] (pRUL1379)	pRS316 with a 1334 bp genomic DNA fragment with *SPL2*	This study
pRS316[NC-SPL2] (pRUL1380)	pRS316 with a 699 bp genomic DNA fragment with the promoter and 5′-end of *SPL2*	This study
YEplac195	Yeast episomal plasmid. *URA3* marker	[62]
YEplac195[BMH1] (pRUL1170)	YEplac195 with a 3.2 kb genomic DNA fragment with *BMH1*	[63]
YEplac195[RRP6] (pRUL1378)	YEplac195 with a 2546 bp genomic DNA fragment with *RRP6*	This study
pRS316[P_{PHO84}-GFP-T_{CYC1}] (pRUL1337)	pRS316 containing the *PHO84* promoter (600 bp), GFP and the *CYC1* terminator (220 bp)	[22]
pRS316[P_{CYC} -GFP-T_{CYC1}] (pRUL1339)	pRS316 containing the *CYC1* promoter (300 bp), GFP and the *CYC1* terminator (220 bp)	[22]
pRS316[P_{SPL2} 1-GFP-T_{CYC1}] (pRUL1356)	pRS316 containing the *SPL2* promoter (647 bp), GFP and the *CYC1* terminator (220 bp)	This study
pRS316[P_{SPL2} 0-GFP-T_{CYC1}] (pRUL1386)	pRS316 containing the *SPL2* promoter (568 bp), GFP and the *CYC1* terminator (220 bp)	This study
pRS316[P_{SPL2}-2-GFP-T_{CYC1}] (pRUL1387)	pRS316 containing the *SPL2* promoter (670 bp), GFP and the *CYC1* terminator (220 bp)	This study
pML104	Plasmid for expression of Cas9 and contains guide RNA expression cassette. *URA3* selection marker.	(John Wyrick; Addgene # 67638) [64]
pML104[P(SPL2)] (pRUL1375)	CRISPR-Cas plasmid for deletion of block P of *SPL2* promoter	This study
pML104[T_{PHO84}::T_{CYC1}] (pRUL1385)	CRISPR-Cas plasmid for replacement of *PHO84* terminator sequences.	This study

2.2. Construction of plasmids

The low copy plasmid pRS316[RRP6] was constructed by ligation of a 2546 bp PCR fragment containing the *RRP6* promoter, coding and terminator sequences into pRS316 after digestion with *Eco*RI and *Hin*dIII. The PCR fragment was obtained by using the primers RRP6-Fw and RRP6-Rev and BY4741 genomic DNA as template. The multicopy plasmid YEplac195[RRP6] was obtained by cloning this PCR fragment into YEplac195 after digestion with *Eco*RI and *Hind*III. Plasmid pRS316 [SPL2] was constructed by ligation of a 1334 bp PCR fragment containing the *SPL2* promoter, coding and terminator sequences into pRS316 after digestion with *Eco*RI and *Sac*I. The PCR fragment was obtained by using the primers P-SPL2-Fw and T-SPL2-Rev and BY4741 genomic DNA as template. Plasmid pRS316[NC-SPL2] was constructed by ligation of a 699 bp PCR containing the *SPL2* promoter and 5′-end of the coding sequences into pRS316 after digestion with *Eco*RI and *Sac*I. The PCR fragment was obtained by using the primers P-SPL2-Fw and

Table 3
Primers.

Primer	Sequence (5′-3′)
SPL2-GFP-Fw2	ATTGACGAAGACATATTCGAAGATTCGTCTGACGAAGAACAATCACGTACGCTGCAGGTCGAC
SPL2-GFP-Rv	GTCAATGCATATGTAACAGTACAGAGGTAGAAGGTATGTGTATCGATGAATTCGAGCTCG
RRP6-Fw	AA AAGCTT CCCAAAAATATGAGGGCATCG
RRP6-Rev	AA GAATTC CGGATAACCTCCGACGTTGAA
P-SPL2-Fw	AAA GAGCTC TTTACACTGGGATATTACAAGAC C
P-SPL2-Rv2	AAA ACTAGT CATCTGTCCAATTTGCCCCTG
P-SPL2-Rv3	AAA ACTAGT CATTTTGCCGCGTGGAGACAT
P-SPL2-Rev-0	AAA ACTAGT CATGGGAAGTCATAGTAATAGATC
T-SPL2-Rev	AAA GAATTC AAAGGGCCAGCGAATGCGCG
NC-spl2-Rv	AAA GAATTC GTTGTCCTTGTGAAACTGCTG
SPL2-NB1	GCATATGTAACAGTACAGAGG
SPL2-NB2	AACATCGCAGTCACAATCTCT
SPL2-NB3	CATGGGAAGTCATAGTAATAGA
SPL2-NB4	CAACGCCGTAAAGTTCCAAAC
ACT1-NB1	CAAGGTATCATGGTCGGTATG
ACT1-NB2	GGGCTCTGAATCTTTCGTTAC
PHO84-NB-Fw	ATGAGTTCCG TCAATAAAGA TAC
PHO84-NB-Rev	TTATGCTTCATGTTGAAGTTGAG
P-repair-1	ATGTTACAACAGTCAAAGTAATGAACTTTCGCCCACGTGCGTACATCATTTACTATCTCAAAAGAGAGAGCCGTACCGCAATAAAATGGACCCTTGTCGGTCACGTGAGCAAAAATACTA
P-repair-2	TAGTATTTTTGCTCACGTGACCGACAAGGGTCCATTTTATTGCGGTACGGCTCTCTCTTTTGAGATAGTAAATGATGTACGCACGTGGGCGAAAGTTCATTACTTTGACTGTTGTAACAT
SPL2-qPCR-4	GCTGTACCGCCAAGGTAGAT
P-gRNA-5	GGGAACAAAAGCTGGAGCTCC
P-gRNA-7	CTAGCTCTAAAACTAACTGCCATGCATTTATGTGATCATTTATCTTTCACTGCGGAG
PHO84-gRNA-1	CTAGCTCTAAAACCAAAGATGCACTAAAACTTGGATCATTTATCTTTCACTGCGGAG
PHO84-CYC1-Fw	ATAATGACATTGAATCTTCCAGCCCATCTCAACTTCAACATGAAGCATAAACAGGCCCCTTTTCCTTTGTC
PHO84-CYC1-Rev	GAAATAATGAAATTAAAAGAAATTATCGAATAAATATGTAACCTGACAGTATGTTACATGCGTACACGCGT
PHO84-qPCR-Fw	ACAACCTTGTTGATCCCAG
T-pho84-Rv2	AAA GAATTCC TATTTGACAACCTGCTTGACC

NC-spl2-Rv and BY4741 genomic DNA as template.

The reporter plasmids pRS316[P_{PHO84}-GFP-T_{CYC1}], pRS316[P_{SPL2} 0-GFP-T_{CYC1}], pRS316[P_{SPL2} 1-GFP-T_{CYC1}], pRS316[P_{SPL2} 2-GFP-T_{CYC1}] and pRS316[P_{CYC1}-GFP-T_{CYC1}] were constructed as described previously [22]. To obtain P_{SPL2} 1 primers P-SPL2-Fw and P-SPL2-Rv2 were used, to obtain P_{SPL2}-0 primers P-SPL2-Fw and P-SPL2-Rev-0 were used and to obtain P_{SPL2}-2 primers P-SPL2-Fw and P-SPL2-Rv3 were used.

For removal of box P from the *SPL2* promoter we made use of the CRISPR-Cas technology. Plasmid pML104 was digested with *Sac*II and *Swa*I and the digested vector was isolated by gel electrophoresis. Guide RNA fragment P was obtained by PCR on undigested pML104 using primers P-gRNA-5 and P-gRNA-7. The guide fragment was digested with *Sac*II and ligated in pML104 digested with *Sac*II and *Swa*I yielding plasmid pML104[P(SPL2)].

For replacement of *PHO84* terminator sequences by *CYC1* terminator sequences using the CRISPR-Cas technology, plasmid pML104 was used. The guide fragment was obtained by PCR on undigested pML104 using primers P-gRNA-5 and PHO84-gRNA-1. The guide fragment was digested with *Sac*II and ligated in pML104 digested with *Sac*II and *Swa*I yielding plasmid pML104[T_{PHO84}::T_{CYC1}].

2.3. Construction of yeast strains

To tag chromosomal *SPL2* at its 3′-end with GFP a PCR fragment was generated using the primer combination SPL2-GFP-Fw2 - SPL2-GFP-Rv and plasmid pYM28 [27] as template. This fragment was used to transform rrp6Δ and pho4Δ yielding the histidine prototrophic strains rrp6Δ SPL2-GFP and pho4Δ SPL2-GFP, respectively. Correct integration was verified by PCR.

For deletion of box P of the *SPL2* promoter by the CRISPR-Cas technique yeast strains were co-transformed with 250 ng of plasmid pML104[P(SPL2)] and 1 μg of the repair fragment and transformants were selected for uracil prototrophy. The repair fragment was obtained by annealing oligo's P-repair-1 and P-repair-2. Transformants are expected to have the required deletion but they still contain the pML104[P(SPL2)] plasmid. The transformants were streaked on a plate containing 5-fluoro-orotic acid (1 mg/mL) and uracil in addition to methionine, histidine and leucine to select for cells that have lost the plasmid. After incubation for 5 days at 30 °C, colonies were taken and plated on plates containing or lacking uracil. Uracil auxotrophic transformants were selected and DNA was isolated. The *SPL2* promoter was analyzed by PCR using primers P-SPL2-Fw and SPL2-qPCR-4 followed by sequencing of the PCR fragments.

For replacement of sequences of the *PHO84* terminator by the CRISPR-Cas technique yeast strains were co-transformed with 250 ng of plasmid pML104[T_{PHO84}::T_{CYC1}] and 1 μg of the replacement fragment and transformants were selected for uracil prototrophy. The replacement fragment was obtained by PCR on BY4741 chromosomal DNA using primers PHO84-CYC1-Fw and PHO84-CYC1-Rev. The transformants were streaked on a plate containing 5-fluoro-orotic acid (1 mg/mL) and uracil in addition to methionine, histidine and leucine to select for cells that have lost the plasmid. After incubation for 5 days at 30 °C, colonies were taken and plated on plates containing or lacking uracil. Uracil auxotrophic transformants were selected and DNA was isolated. The *PHO84* terminator was analyzed by PCR using primers PHO84-qPCR-Fw and T-pho84-Rv2, followed by sequencing of the PCR fragments.

2.4. Transcriptome analysis by strand-specific RNAseq

Cultivation of yeast strains and isolation of RNA was done as described previously [28]. RNAseq was performed by BaseClear (Leiden, the Netherlands). The dUTP method was used to generate strand-specific mRNA-seq libraries including barcoding [29]. The Illumina TruSeq stranded RNA-seq library preparation kit is used and the purified mRNA is fragmented and converted to double-stranded cDNA. DNA adapters with sample-specific barcodes are ligated and a PCR amplification is performed. The library is size-selected using magnetic beads, resulting on average in libraries with insert size in the approximate range of 100–400 bp and sequenced on the Illumina HiSeq 2500. At least 20 million reads were obtained for each sample.

Sequence reads were analyzed using CLC Genomic Workbench software. The reference sequences were downloaded from SGD (www.yeastgenome.org). Alignment files (.sam files) were displayed using Tablet [30]. Statistical analyses were done with the EdgeR package in R [31].

For BY4741 three independent cultures cultivated at 7.2 mM potassium phosphate and three independent cultures cultivated without phosphate were used. For spl2Δ three independent cultures cultivated at 7.2 mM potassium phosphate and two independent cultures cultivated without phosphate were used. For bmh1Δ one culture cultivated at 7.2 mM potassium phosphate was used. For rrp6Δ RNAseq was done in a separate experiment including two independent cultures of rrp6Δ and one culture of BY4741 cultivated at 7.2 mM potassium phosphate. For studying the effect of deletion of box P of the *SPL2* promoter a separate experiment was conducted with one culture of BY4741 and one culture of BY4741 ΔP, cultivated at 7.2 mM potassium phosphate. The raw sequence data have been deposited in NCBI's Gene Expression Omnibus (GEO) and is accessible through GEO Series accession number GSE135911. All normalized read counts are shown in Supplementary Table S6.

2.5. Northern blot analysis

Total RNA was isolated as described [32] and 20 μg RNA of each sample was used for Northern blot analysis as described [33]. The indicated probes were prepared by PCR and subsequently labeled with [α-^{32}P]dCTP by random-primed DNA synthesis using the Random Primers DNA Labeling System (Invitrogen) kit.

2.6. Confocal microscopy and flow cytometry

Yeast cells were grown in phosphate-free YNB medium supplemented with KCl, potassium phosphate, histidine, methionine, uracil and leucine, when required. For image acquisition a Zeiss LSM 5 Exciter-AxioImager M1 confocal microscope with a Plan-Apochromat objective (63×/1.4 Oil DIC) and Zeiss ZEN 2009 software were used. GFP was imaged with excitation at 488 nm and emission at 505–600 nm. ImageJ (National Institute of Health) [34] was used to increase the visibility of the GFP signals and cells by linear adjustments of intensities. For flow cytometry, a Merck-Millipore Guava EasyCyte 5 Flow Cytometer was used. Fluorescence was determined after excitation at 488 nm and using the standard green 525/30 nm emission filter. For each analysis 5000 cells were used.

3. Results

3.1. Deletion of BMH1 reduces SPL2 and PHO84 expression

In our previous study [22] we showed that deletion of *BMH1* resulted in a strongly reduced level of *PHO84* and *SPL2* mRNA. To further study the effect of the *BMH1* deletion on the transcription of genes involved in phosphate homeostasis we analyzed the effect of the *BMH1* deletion on genome-wide transcription using strand-specific RNAseq instead of using Serial Analysis of Gene Expression (SAGE)-tag sequencing. As shown in Table 4, the most strongly down-regulated genes are the *PHO* genes *SPL2* (8.1-fold) and *PHO84* (5.6-fold). Other *PHO* genes, like *PHO5* (1.3-fold reduced) are less affected (for complete data set see Supplementary Table S1). Thus, despite the bmh1Δ strain still contains *BMH2*, the absence of *BMH1* strongly reduces the level of *SPL2* and *PHO84* RNA and the effect is rather specific for these two genes and is not an effect on all *PHO* genes. Decreased expression of *SPL2* in the

bmh1Δ strains at standard conditions was confirmed by Northern blotting. As shown in Fig. 1 (SPL2 probe B) a clear band hybridizing to the *SPL2* probe was observed for the wild type strain BY4741, but *SPL2* RNA was hardly detectable in the bmh1Δ strain. The intensity of the bands strongly increased upon starvation for phosphate for 60 min for both BY4741 and bmh1Δ, in line with our previous observations [22] indicating that *SPL2* can still be expressed in the bmh1Δ strain under starvation conditions.

To further analyze the effect of the *BMH1* deletion on the transcription of *SPL2* and *PHO84*, the strand-specific RNAseq reads were aligned to the genomic DNA sequences of these genes. As shown in Fig. 2A, most of the *PHO84* RNAseq reads of the wild type strain BY4741 aligned in the sense direction, and few reads aligned in the antisense direction. On the other hand, almost all of the *PHO84* RNAseq reads of the bmh1Δ strain aligned in the antisense direction (Fig. 2B), and hardly any reads aligned in the sense direction, in line with the strongly reduced levels of *PHO84* RNA in the bmh1Δ strain (Table 4). The number of reads aligning in the sense direction increased upon phosphate starvation (Fig. 2E). Quantification of the reads aligning in the antisense direction showed that the number of antisense reads was not altered by the *BMH1* deletion (20.6 reads per million reads in bmh1Δ *vs.* 21 ± 3, n = 3, reads per million reads in the BY4741 strain) (Table 5), suggesting a minor role of antisense RNA in the regulation of sense transcription by Bmh1p. On the other hand, upon phosphate starvation the number of *PHO84* antisense reads strongly decreased (3.5 ± 0.5, n = 3, reads per million reads). In the BY4741 strain the *SPL2* RNAseq reads aligned almost exclusively in the sense direction. However, only few reads aligned to the 5′-end of the gene, suggesting that this part of the gene is poorly transcribed (Fig. 2A). The number of reads aligning to the coding region of *SPL2* is strongly reduced in the bmh1Δ mutant. However, the remaining reads aligned equally over the 5′- and 3′-parts of the gene. Hardly any reads aligned in the antisense direction. The number of reads aligning to the 3′-part of *SPL2* strongly increased upon phosphate starvation (Fig. 2E).

3.2. Deletion of RRP6 reduces SPL2 and PHO84 expression and results in heterogeneity of SPL2 expression

It has well been established that deletion of *RRP6*, encoding an exonuclease involved in degradation of non-coding RNA [35,36], affects *PHO84* expression [15–17]. To further study the role of non-coding RNA in the regulation of the *PHO* genes we cultivated the rrp6Δ deletion strain under our standard cultivation conditions and performed strand-specific RNAseq analysis. As shown in Supplementary Table S2, 152 genes were significantly up-regulated at least 2.0-fold and 25 genes were significantly down-regulated at least 2.0-fold. *PHO84* sense RNA levels are 3.8-fold lower in the rrp6Δ strain than in BY4741 in agreement with published data. The levels of *SPL2* sense RNA were 2.8-fold lower in the rrp6Δ strain, suggesting regulation of *SPL2* by non-coding RNA. Decreased levels of *SPL2* RNA in rrp6 mutants were observed before [15]. As shown in Fig. 2C, the *PHO84* RNAseq reads of the rrp6Δ strain aligned in both the sense and antisense direction to the *PHO84* gene, with a lower number of reads aligning in the sense direction compared to the wild type. Quantification of the reads aligning in the antisense direction showed that the number of antisense reads was similar as in the wild type strain (23 ± 4, n = 3, reads per million reads in rrp6Δ *vs.* 21 ± 3, n = 3, reads per million reads in the BY4741 strain) (Table 5). The *SPL2* RNAseq reads of the rrp6Δ strain aligned in the sense direction, with almost equal alignment to the 5′- and 3′-parts of the gene, like what was found for the bmh1Δ strain.

In our previous study we showed that deletion of *BMH1* not only resulted in a strongly reduced transcription of *PHO84* and *SPL2*, but also in heterogeneity in the expression of these genes. When phosphate is available, in BY4741 approx. 90% of the cells were expressing *SPL2*-GFP, whereas in the bmh1Δ strain only 20–30% of the cells were expressing *SPL2*-GFP. To investigate a possible role of non-coding RNA in the cell-to-cell variation of the expression of *SPL2*-GFP, we tagged *SPL2* with GFP in the rrp6Δ deletion mutant. As shown in Fig. 3C, more than half of the rrp6Δ SPL2-GFP cells were not expressing *SPL2*-GFP, similar as observed for the bmh1Δ SPL2-GFP cells (Fig. 3B). In contrast, most cells of BY4741 SPL2-GFP were expressing *SPL2*-GFP (Fig. 3A). As shown in Fig. 3H, addition of a wild type copy of *RRP6* (pRS316RRP6) to

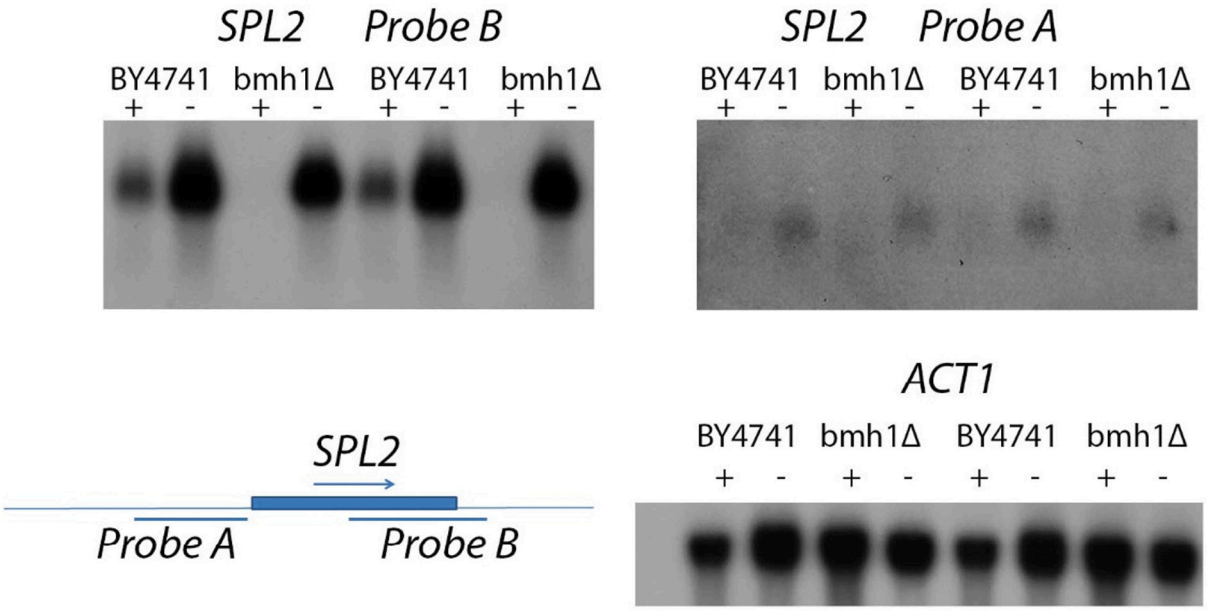

Fig. 1. Northern blot analysis of *SPL2* RNA isolated from BY4741 and bmh1Δ cells grown at standard phosphate concentrations and after 60 min phosphate starvation. Total RNA was isolated from exponentially growing cultures (A_{620} of 0.5) in YNB with 7.2 mM potassium phosphate (+) or grown for 60 min in YNB medium lacking phosphate (−). Probes were made by PCR, followed by labeling with [α-^{32}P]dCTP. PCR Primers used: SPL2 Probe B, SPL2-NB1 and SPL2-NB2; SPL2 Probe A, SPL2-NB3 and SPL2-NB4; ACT1, ACT1-NB1 and ACT1-NB2. Blots hybridized to the *SPL2* probes were aligned based on non-specific hybridization on an unspecified RNA marker.

Table 4
Genes of which the RNA levels were significantly (FDR < 0.01) decreased more than 2.0-fold in the bmh1Δ strain compared to BY4741 after culturing in supplemented YNB-medium containing 7.2 mM potassium phosphate.

Gene	Function	Fold decrease	Probability (P)
BMH1	14-3-3 protein, major isoform	(807.5)	2.79E−211
SPL2	Protein with similarity to cyclin-dependent kinase inhibitors; downregulates low-affinity phosphate transport	8.1	2.77E−09
PHO84	High-affinity inorganic phosphate (Pi) transporter	5.6	9.23E−17
HXT4	High-affinity glucose transporter	3.4	0.00047
PHM6	Protein of unknown function; expression is regulated by phosphate levels	2.9	6.40E−05
AGA1	Anchorage subunit of a-agglutinin of a-cells	2.9	0.00041
YHB1	Nitric oxide oxidoreductase	2.8	5.49E−08
YLR227W-B	Retrotransposon TYA Gag and TYB Pol genes	2.6	0.00031
BAT2	Cytosolic branched-chain amino acid aminotransferase	2.5	1.49E−14
VTC3	Regulatory subunit of the vacuolar transporter chaperone complex	2.3	0.00030
DDR48	DNA damage-responsive protein	2.3	1.34E−07
OYE2	Conserved NADPH oxidoreductase containing flavin mononucleotide	2.2	2.23E−23
SFG1	Nuclear protein putative transcription factor	2.2	0.00018
GRE2	3-methylbutanal reductase and NADPH-dependent methylglyoxal reductase	2.0	0.00012
Selected PHO genes			
PHO89	Plasma membrane Na+/Pi cotransporter	2.1	0.40
PHO5	Repressible acid phosphatase	1.3	0.41
PHO11	One of three repressible acid phosphatases	1.3	0.35
PHO12	One of three repressible acid phosphatases	2.2	0.0012

the rrp6Δ SPL2-GFP cells resulted in expression of *SPL2*-GFP in almost all cells, whereas addition of the empty vector (pRS316) had little effect (Fig. 3G). Analysis of the cells by flow cytometry (Fig. 3I and J) confirmed this observation, indicating that deletion of *RRP6* is responsible for the lower number of cells expressing *SPL2*-GFP, suggesting a role of non-coding transcription in the cell-to-cell variation of *SPL2*-GFP expression. In the pho4Δ mutant expression of *SPL2-GFP* could not be detected, indicating an essential role of Pho4 in the expression of *SPL2* (Fig. 3D).

To further investigate the relationship between the effect of the *bmh1* and *rrp6* deletions on the expression of *SPL2-GFP* we introduced *BMH1* and *RRP6* on the multicopy plasmid YEplac195 in the BY4741 SPL2-GFP, bmh1Δ SPL2-GFP and rrp6Δ SPL2-GFP strains. As shown in Fig. 4 introduction of YEplac195[BMH1] allowing overexpression of *BMH1* increased *SPL2-GFP* expression in all three strains. However, overexpression of *BMH1* in rrp6Δ SPL2-GFP still resulted in a lower expression of *SPL2-GFP* than after overexpression of *BMH1* in BY4741 SPL2-GFP, indicating that the effect of the *RRP6* deletion cannot completely be suppressed by overexpression of *BMH1*. Introduction of *RRP6* on the multicopy plasmid has little effect in all three strains, except in the rrp6Δ SPL2-GFP strain. The latter effect may be in part due to complementation of the deletion, although *SPL2-GFP* expression is not as high as in the wild type strain.

3.3. Spl2 stimulates its own expression and that of PHO84

In our previous study we observed Spl2-GFP in cellular structures resembling the nucleus [22]. A nuclear localization of Spl2 may indicate a role of Spl2 in transcriptional regulation. To investigate possible involvement of Spl2 in transcriptional regulation, we analyzed genome-wide transcription in a spl2Δ deletion mutant by strand-specific RNAseq (for complete data set see Supplementary Table S3). The effect of *SPL2* disruption on the transcriptome was very limited, only one gene (YGR109W-B, a transposable element gene) was significantly up-regulated more than 2.0-fold, and four genes (*PHO84*, *PHM6*, *PHO12* and *VTC3*) were significantly down-regulated more than 2.0-fold. The latter genes are related to phosphate uptake and the strongest decrease, except for *SPL2*, was found for *PHO84* (6.1-fold). Alignment of the RNAseq reads to the genomic sequences of *SPL2* showed the absence of alignment to the *SPL2* coding region, as expected due to the deletion (Fig. 2D). Alignment of the RNAseq reads to *PHO84* showed almost exclusively alignment in the antisense direction (Fig. 2D). However, quantification of the antisense reads showed no significant difference with the wild type: 25 ± 2, $n = 2$, reads per million align in the antisense direction in spl2Δ *vs.* 21 ± 3, $n = 3$, reads per million in BY4741 (Table 5).

To investigate the effect of the bmh1Δ, rrp6Δ and spl2Δ deletion on the activity of the *PHO84* and *SPL2* promoter rather than on the RNA level, we inserted the promoter sequences of these genes upstream of GFP in the pRS316 plasmid. The coding region of *SPL2* may be different from the annotated coding region. Very close to the annotated start codon ATG is an upstream out of frame ATG, making it less likely that the annotated start codon is the correct start codon as mentioned before [21] (Supplementary Fig. S1A). Genome-wide studies on the transcriptional start sites suggest that the second downstream ATG may be the actual start codon for *SPL2* translation [37]. To further investigate the *SPL2* start codon, we used promoter sequences corresponding to the annotated start codon, to the first downstream ATG and to the second downstream ATG. As shown in Supplementary Fig. S1B, hardly any GFP expression was found using the promoter construct (P_{SPL2} 0) corresponding to the annotated start codon. The highest expression was observed for the promoter construct corresponding to the second downstream ATG (P_{SPL2} 2). Therefore, we used this construct for further studies. The constructed plasmids were introduced into BY4741 and the various deletion mutants and GFP fluorescence was determined by flow cytometry in exponentially growing cells. As shown in Fig. 5 the activity of the *SPL2* and *PHO84* promoter is lower in the bmh1Δ, rrp6Δ and spl2Δ deletion mutants, whereas the *CYC1* promoter was hardly affected. Thus, the activity of the *PHO84* and *SPL2* promoter is not only affected by the *bmh1* deletion, but also by the *spl2* and *rrp6* deletions. These results suggest that *SPL2* stimulates its own expression and that of *PHO84*.

To further investigate the possible self-stimulation of *SPL2* an additional copy of *SPL2* was introduced in BY4741 SPL2-GFP and rrp6Δ SPL2-GFP by transformation with plasmid pRS316[SPL2] containing *SPL2* including its own promoter and terminator. As shown in Fig. 6A and B there was no significant effect on the expression of *SPL2-GFP* in BY4741, whereas *SPL2-GFP* expression is strongly stimulated in the rrp6Δ background. Flow cytometry showed a decreased number of cells not expressing *SPL2-GFP* upon addition of an extra copy of *SPL2* both in the BY4741 and rrp6Δ background (Fig. 6D and E, respectively). Similar observations were made by confocal microscopy (Fig. 6G and J, BY4741 background; Fig. 6H and K, rrp6Δ background).

As *SPL2* deletion strongly reduced *PHO84* expression we investigated the effect of an additional copy of *SPL2* on the activity of the *PHO84* promoter. To this end, *SPL2* on the low copy plasmid pRS316 (pRS316 [SPL2]) was introduced into the strain in which GFP under control of the *PHO84* promoter was integrated in the *leu2* locus (BY4741 (P_{PHO84}-GFP)). As shown in Fig. 6 (C, F, I and L) an additional copy of *SPL2* stimulated the activity of the *PHO84* promoter almost 10-fold.

To investigate the role of *SPL2* in gene expression during phosphate starvation conditions, we analyzed the effect of phosphate starvation for 60 min on the transcriptome of both BY4741 and spl2Δ strains. As

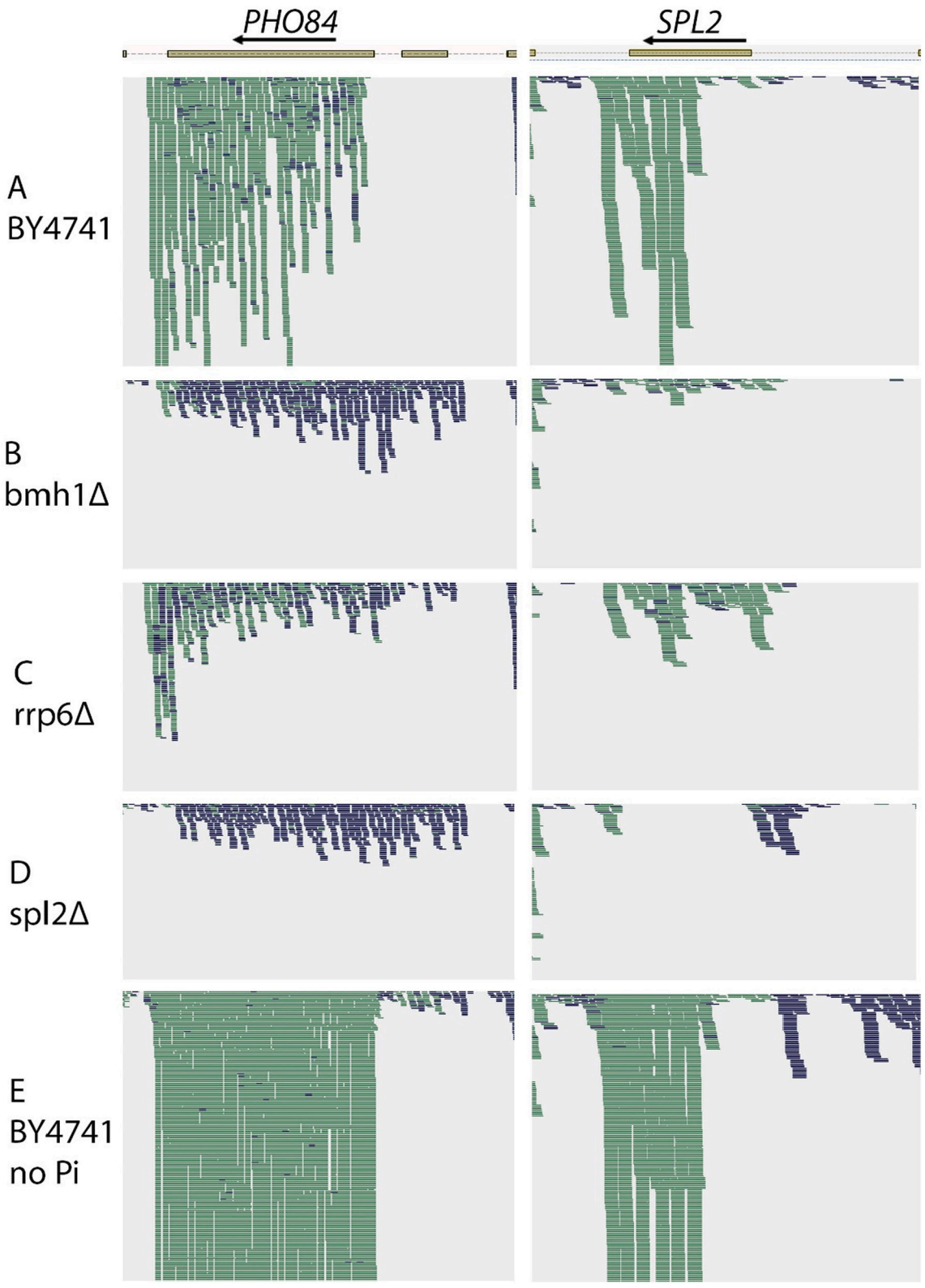

Fig. 2. Alignment of strand-specific RNAseq reads to genomic sequences of *PHO84* and *SPL2*. Genomic sequences (S288c) were taken from SGD (www.yeastgenome.org). Reads were aligned using CLC Genomic Workbench and alignments were visualized using Tablet. Reads corresponding to the Watson-strand (left to right) are indicated in blue, reads corresponding to the Crick strand (right to left) are indicated in green. Both *PHO84* and *SPL2* coding regions are located on the Crick strand.

shown in Supplementary Table S4 in BY4741 RNA levels of 38 genes were significantly at least 2.0-fold increased upon phosphate starvation and the levels of 4 genes were decreased at least 2.0-fold. In the spl2Δ deletion mutant the RNA levels of 26 genes were increased and that of 15 genes were decreased (Supplementary Table S5). *PHO* genes including *PHO84* and *PHO5* were still upregulated in the spl2Δ strain upon phosphate starvation. These results indicate that the induction of gene expression in response to phosphate starvation is not affected by

Table 5
Number of reads aligning in the antisense direction to *PHO84*.

Strain	Number of reads per million reads
BY4741	21 ± 3 (n = 3)[a]
bmh1Δ	20.6 (n = 1)
rrp6Δ	23 ± 4 (n = 3)
spl2Δ	25 ± 2 (n = 2)
BY4741 without phosphate	3.5 ± 0.5 (n = 3)

[a] The average with standard deviation with the number of replicates in parentheses is shown.

the *SPL2* deletion. The number of antisense *PHO84* reads strongly decreased upon phosphate starvation in both BY4741 and the spl2Δ strain (3.4 ± 0.3, n = 3, reads per million for spl2Δ and 3.5 ± 0.5, n = 3, reads per million for BY4741).

3.4. The effect of the bmh1 and rrp6 deletion is not related to antisense PHO84 transcription

It has been shown before that *PHO84* expression is regulated by antisense transcription [15–17]. Therefore, we further tested whether the effect of the *BMH1* and *RRP6* deletions is *via* antisense transcription. To study the activity of the *PHO84* and *SPL2* promoters in these mutants we inserted the promoter sequences of *PHO84* and *SPL2* upstream of GFP in the pRS316 plasmid (pRS316[P_{PHO84}-GFP-T_{CYC1}]) and showed that the activity of the promoters was strongly decreased (Fig. 5). The used plasmids contain the terminator sequences of *CYC1* and not the terminator sequences of *PHO84* or *SPL2*. Alignment of antisense RNAseq

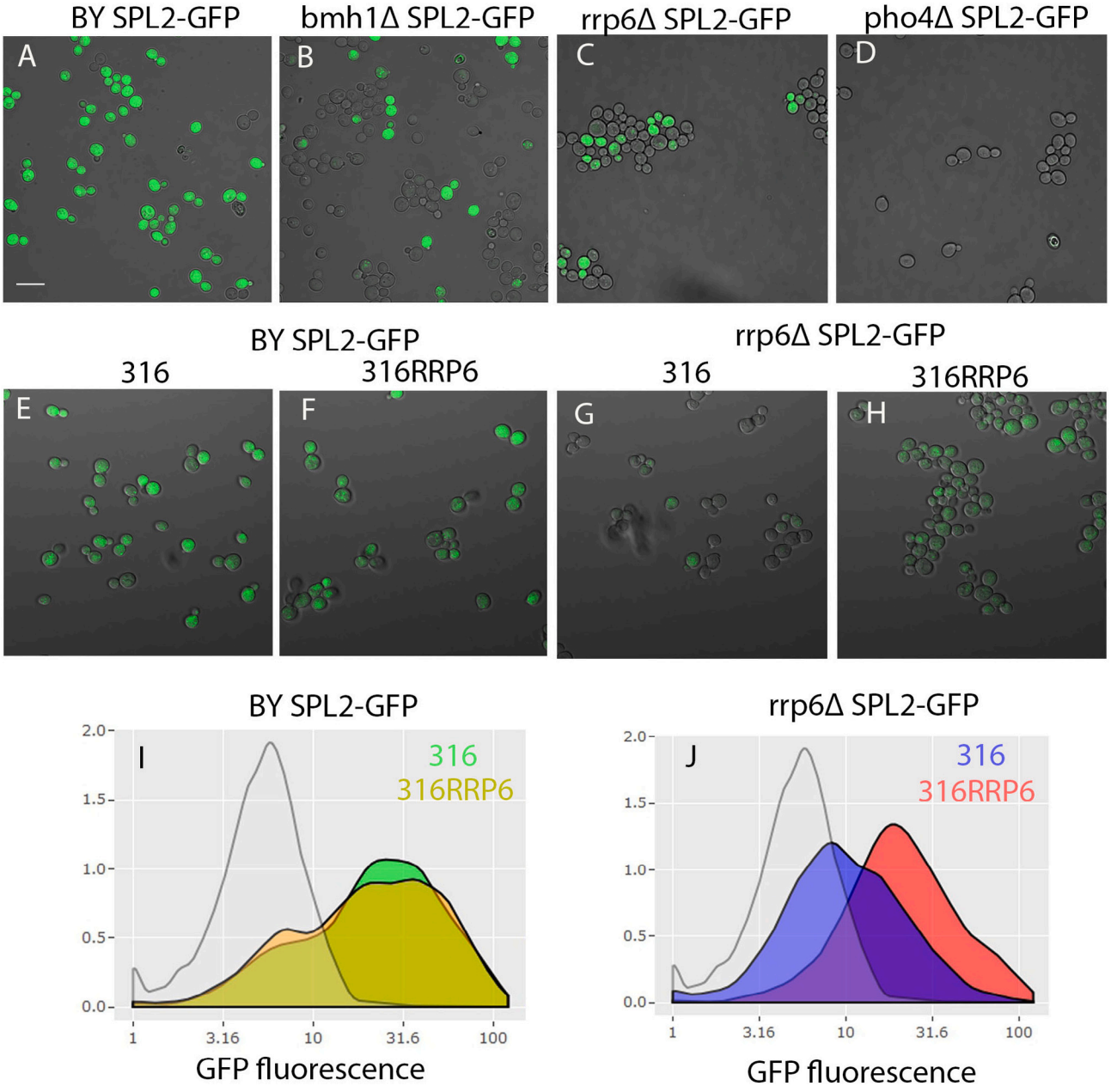

Fig. 3. Effect of deletion of *RRP6* on the heterogeneity in *SPL2-GFP* expression. Microscopy images of BY4741 SPL2-GFP (A), bmh1Δ SPL2-GFP (B), rrp6 Δ SPL2-GFP (C), pho4Δ SPL2-GFP (D), BY4741 SPL2-GFP pRS316 (E), BY4741 SPL2-GFP pRS316[RRP6] (F), rrp6Δ SPL2-GFP pRS316 (G) and rrp6Δ SPL2-GFP pRS316[RRP6] (H) after growth in YNB medium supplemented with potassium and phosphate. Flow cytometry of BY4741 (I and J, no fill), BY4741 SPL2-GFP pRS316 (I, green), BY4741 SPL2-GFP pRS316[RRP6] (I, orange), rrp6Δ SPL2-GFP pRS316 (J, blue) and rrp6Δ SPL2-GFP pRS316[RRP6] (J, red). Results of a typical experiment are shown.

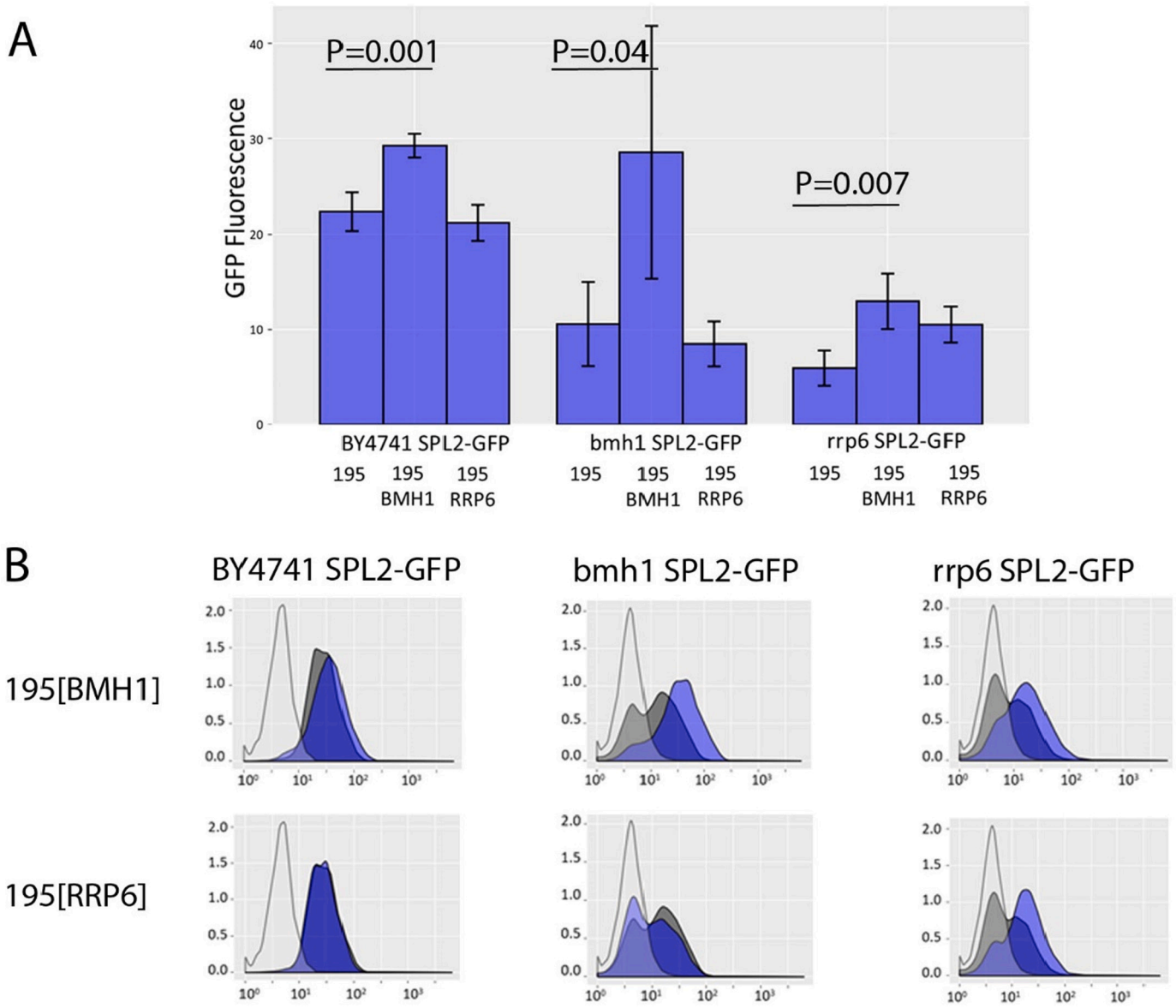

Fig. 4. Effect of YEplac195[BMH1] or YEplac195[RRP6] on *SPL2-GFP* expression in BY4741, bmh1Δ and rrp6Δ strains. The indicated strains were grown in YNB medium supplemented with potassium and phosphate and GFP fluorescence was measured by flow cytometry. A. Average GFP fluorescence with standard deviation of measurements on four independent transformants. Statistical analysis was performed with the Student's *t*-test, and the significance (P) of the difference between strains with the empty YEplac195 vector (195) and YEplac195[BMH1] (195BMH1) is indicated. The difference between strains with the empty YEplac195 vector (195) and YEplac195[RRP6] (195RRP6) was not significant. B. Flow cytometry graphs of one series of transformants. Blue, transformant containing YEplac195 [BMH1] or YEplac195[RRP6], as indicated; Gray, transformant containing YEplac195; open graph, BY4741.

reads to *PHO84* suggests that *PHO84* terminator sequences are responsible for the antisense transcription. This suggests that antisense *PHO84* transcription is not causing the reduced activity of the sense promoter in the mutants. On the other hand, the endogenous *PHO84* gene is still present in the mutants and a *trans* effect of the chromosomal antisense transcripts on the promoter in the plasmid cannot be excluded [38]. To eliminate chromosomal *PHO84* antisense transcription we replaced 96 bp of the chromosomal sequences immediately downstream of the *PHO84* stop codon by 220 bp of the *CYC1* terminator using the CRISPR-Cas technology. If a *trans* inhibitory effect occurs, it is expected that replacement of the *PHO84* terminator sequences results in increased GFP levels. As shown in Supplementary Fig. S2 GFP levels were strongly decreased rather than increased in the strain lacking the *PHO84* terminator sequences, indicating that it is very unlikely that under the applied growth conditions the *PHO84* or the *SPL2* promoter is inhibited by *PHO84* antisense RNA in a *trans* fashion. Similar effects were observed after replacement of the *PHO84* terminator sequences in the bmh1Δ, rrp6Δ and spl2Δ strains (Supplementary Fig. S2).

3.5. Deletion of the putative start site of upstream SPL2 transcription results in loss of heterogeneity of SPL2 expression and increased PHO84 expression

Alignment of RNAseq reads to the *SPL2* genomic sequences suggests different transcription start sites (Fig. 2). It has been reported that non-coding RNA transcribed from an alternative upstream start site regulates transcription of the coding sequences of the meiosis genes *NDC80*, *IME1* and *BOI1* [39–42]. Alignment of the RNAseq reads of the wild type strain BY4741 and the rrp6Δ mutant to the *SPL2* genomic sequences are shown in more detail in Fig. 7A. The alignment profiles may be explained by two major transcriptional start sites resulting in different RNAs as illustrated by a blue and red arrow in Fig. 7A. To investigate the

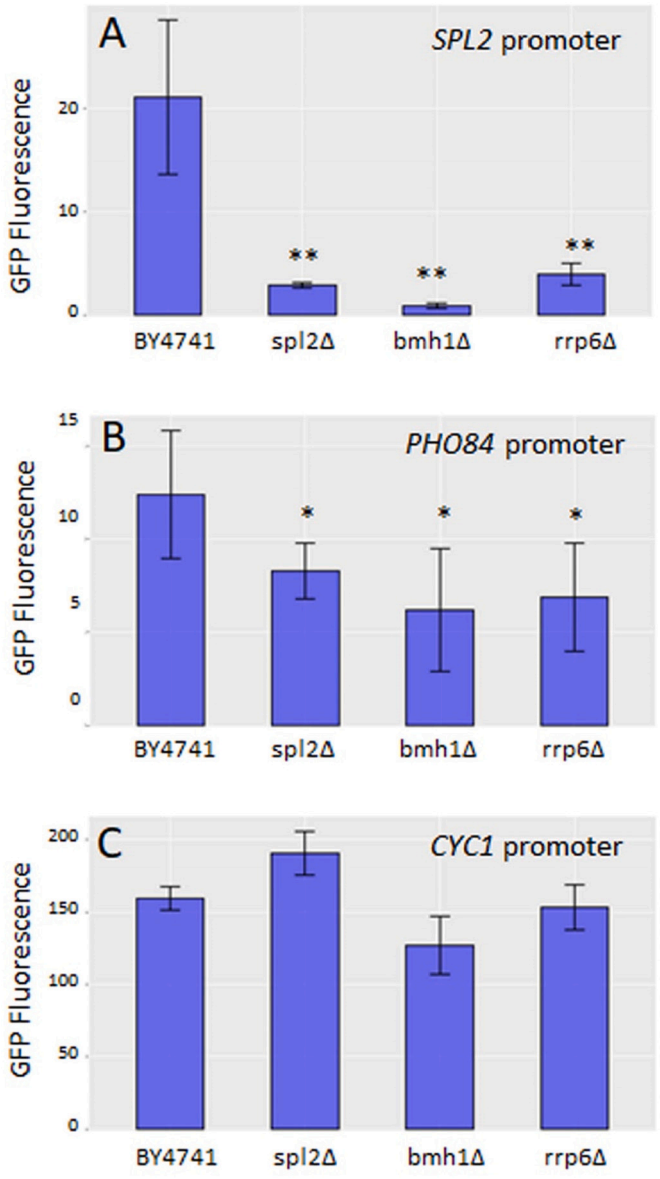

Fig. 5. Effect of deletion of *SPL2*, *BMH1* and *RRP6* on the activity of the *SPL2*, *PHO84* and *CYC1* promoter. The reporter plasmids pRS316[P_{PHO84}-GFP-T_{CYC1}], pRS316[P_{SPL2}-GFP-T_{CYC1}] and pRS316[P_{CYC1}-GFP-T_{CYC1}] were introduced in the indicated yeast strains. The obtained strains were grown in in YNB medium supplemented with potassium and phosphate and GFP fluorescence was measured by flow cytometry. The data shown are the average with standard deviation of measurements on six independent transformants. Statistical analysis was performed with the Student's t-test, and the significance (P) of the difference between the deletion mutant and BY4741 with the same reporter plasmid is shown *, $P < 0.02$, **, $P < 10^{-5}$.

relevance of the upstream transcription we deleted 147 bp around the putative transcription start site by the CRISPR-Cas technology (Fig. 7A, box P). Adjacent to the *SPL2* promoter a number of putative binding sites for the Pho4 transcription factor (5′-CACGTG-3′) [43] were found [44] as illustrated in Fig. 7A by yellow blocks. These binding sites remained unaffected by the deletion. Analysis by confocal microscopy and flow cytometry showed that deletion of box P in BY4741 SPL2-GFP resulted in a loss of the heterogenic expression of *SPL2-GFP* and a more uniform expression of *SPL2-GFP* in the individual cells (Fig. 7B–D). This is more clearly shown upon deletion of box P in bmh1 SPL2-GFP (Fig. 7E–G). Similarly, deletion of the box P in rrp6 SPL2-GFP resulted in a low *SPL2-GFP* expression in all cells instead of a heterogenic expression with the majority of the cells not expressing *SPL2-GFP* (Fig. 7H–J). These results indicate that the deleted part of the *SPL2* promoter has a negative effect on the expression of *SPL2*, at least in the BY4741 and bmh1 background, and that upstream non-coding transcription may be responsible for the heterogenic expression of *SPL2*.

As Spl2 influences the expression of *PHO84* we also deleted box P in the BY4741 (P_{PHO84}-GFP) strain, expressing GFP under control of the *PHO84* promoter. Analysis by flow cytometry showed that in the untransformed strain the *PHO84* promoter is active in almost all cells, but is highly active in a small number of cells (Fig. 8A, gray curve). Deletion of box P of the *SPL2* promoter resulted in a much higher number of cells with a very active *PHO84* promoter (Fig. 8A, blue curve). Similar observations were made by microscopic analysis of the cells (Fig. 8B and C). These observations indicate that deletion of box P of the *SPL2* promoter not only affects the expression of *SPL2* but also that of *PHO84*. Addition of a pRS316 plasmid containing the region of the *SPL2* promoter corresponding to the upstream non-coding transcript and lacking the *SPL2* coding sequences (pRS316[NC-SPL2]), did not result in an increased activity of the *PHO84* promoter (Supplementary Fig. S3). This indicates that increased *PHO84* expression is probably not caused by an increased level of non-coding RNA originating from the *SPL2* promoter nor by an increased level of a putative small protein encoded by this RNA but rather by an increased level of the Spl2 protein.

To show whether deletion of box P indeed affects upstream *SPL2* transcription we deleted box P in BY4741 and analyzed transcription by strand-specific RNAseq. As shown in Fig. 9A, upon deletion of box P in BY4741 (BY4741 ΔP) no upstream *SPL2* transcripts were found, whereas it was detectable in BY4741 although at a low level. This result indicates that deletion of box P from the *SPL2* promoter results in the absence of the upstream transcript. No major changes in the alignment of RNAseq reads to *PHO84* were found upon deletion of box P, although deletion of box P resulted in an increased number of reads aligning to the *PHO84* open reading frame (354 *vs.* 249 reads per million; Fig. 9B), in line with the increased activity of the *PHO84* promoter upon deletion of box P in strain BY4741 (P_{PHO84}-GFP) (Fig. 8). Also the number of reads aligning to the *SPL2* open reading frame increased modestly (34 *vs.* 24 reads per million; Fig. 9).

The effect of deletion of box P on the *SPL2* and *PHO84* transcripts was further investigated by Northern blot analysis. As shown in Fig. 9C, the *SPL2* probe (probe B, see Fig. 1) hybridizes to RNA of approximately 600 nucleotides, slightly larger that found observed before (approx. 500 nucleotides [52]). The amount of RNA hybridizing to this probe was strongly increased after deletion of box P, both in BY4741 and in rrp6Δ. A similar effect was observed for RNA hybridizing to the *PHO84* probe. These results are in line with the effect of deletion of box P found by measuring the expression of *SPL2-GFP* (Fig. 7). We did not observe hybridization when we used a probe corresponding to sequences upstream of the *SPL2* coding region (probe A, see Fig. 1), probably due to the lack of sensitivity of the probe used.

4. Discussion

In *S. cerevisiae* phosphate homeostasis is regulated by an interplay between low and high affinity phosphate transporters allowing survival at different environmental phosphate concentrations; for review see [3–5,7]. Expression of these transporters at different phosphate concentrations is regulated by a complex network with a major role for the transcription factor Pho4. Upon phosphate starvation intracellular phosphate levels decrease resulting in inactivation of the Pho80 – Pho85 complex and the Pho4 transcription factor becomes de-phosphorylated and enters the nucleus resulting in expression of more than 20 genes (*PHO* genes) necessary for growth and survival at low phosphate conditions. Under these conditions genes encoding the high affinity phosphate transporters Pho84 [12] and Pho89 [45] are expressed. Furthermore, *SPL2* is expressed to target the low affinity phosphate transporter Pho87 to the vacuole [14]. When phosphate is abundant low

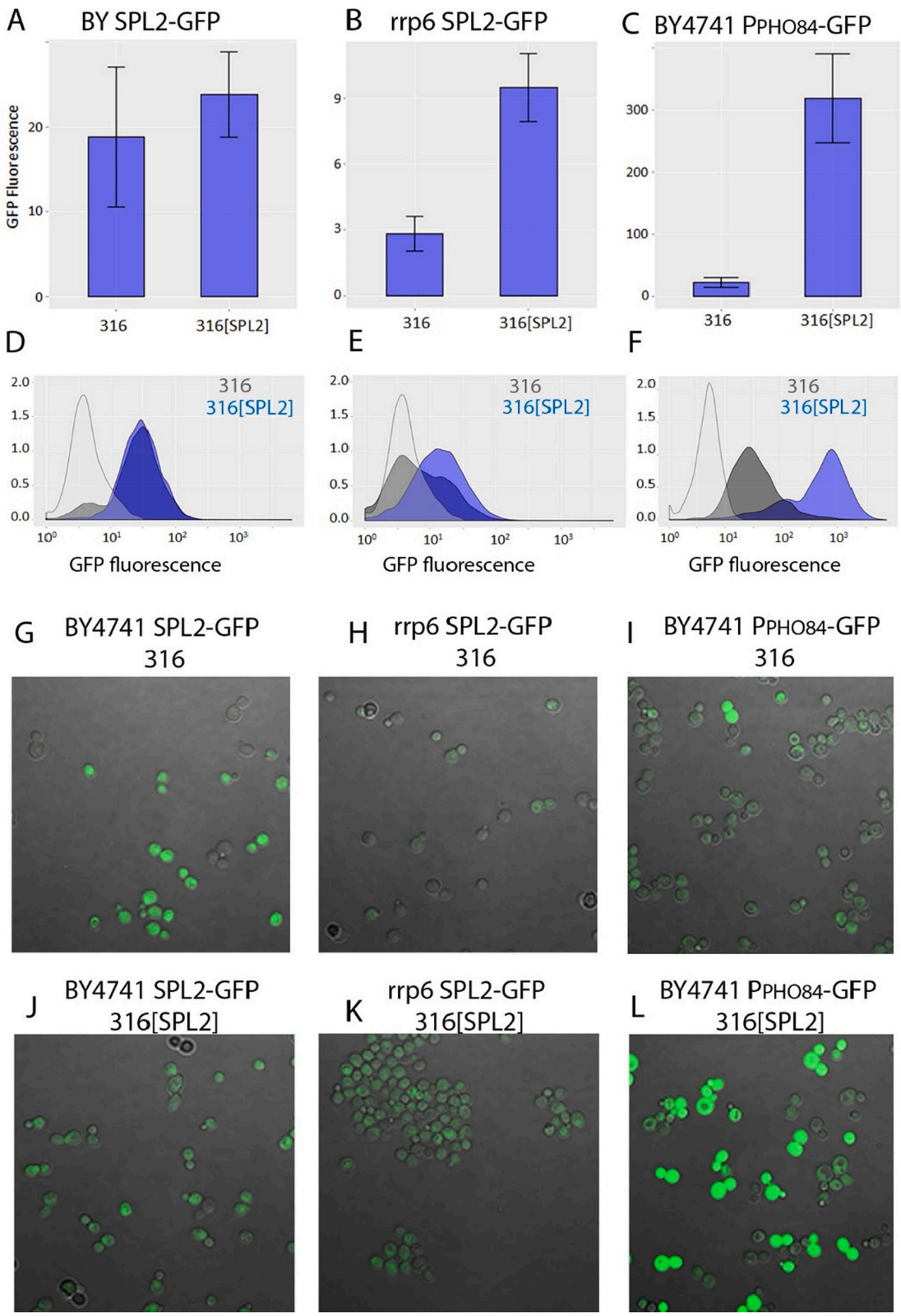

Fig. 6. Effect of an additional copy of *SPL2* on the expression of *SPL2-GFP* and the activity of the *PHO84* promoter. A, SPL2-GFP fluorescence of BY4741 SPL2-GFP containing pRS316 or pRS316[SPL2] (mean ± SD, n = 8). B, SPL2-GFP fluorescence of rrp6Δ SPL2-GFP containing pRS316 or pRS316[SPL2] (mean ± SD, n = 8). C, GFP fluorescence of BY4741 (P_{PHO84}-GFP) containing pRS316 or pRS316[SPL2] (mean ± SD, n = 6). D, flow cytometry of BY4741 (no fill), BY4741 SPL2-GFP pRS316 (gray) and BY4741 SPL2-GFP pRS316[SPL2] (blue). E, flow cytometry of BY4741 (no fill), rrp6Δ SPL2-GFP pRS316 (gray) and rrp6Δ SPL2-GFP pRS316 [SPL2] (blue). F, flow cytometry of BY4741 (no fill), BY4741 (P_{PHO84}-GFP) pRS316 (gray) and BY4741 (P_{PHO84}-GFP) pRS316[SPL2] (blue). D–F, results of a typical experiment are shown; 5000 cells were analyzed. G–L, confocal microscopy of BY4741 SPL2-GFP pRS316 (G), rrp6Δ SPL2-GFP pRS316 (H), BY4741 (P_{PHO84}-GFP) pRS316 (I), BY4741 SPL2-GFP pRS316[SPL2] (J), rrp6Δ SPL2-GFP pRS316[SPL2] (K) and BY4741 (P_{PHO84}-GFP) pRS316[SPL2] (L).

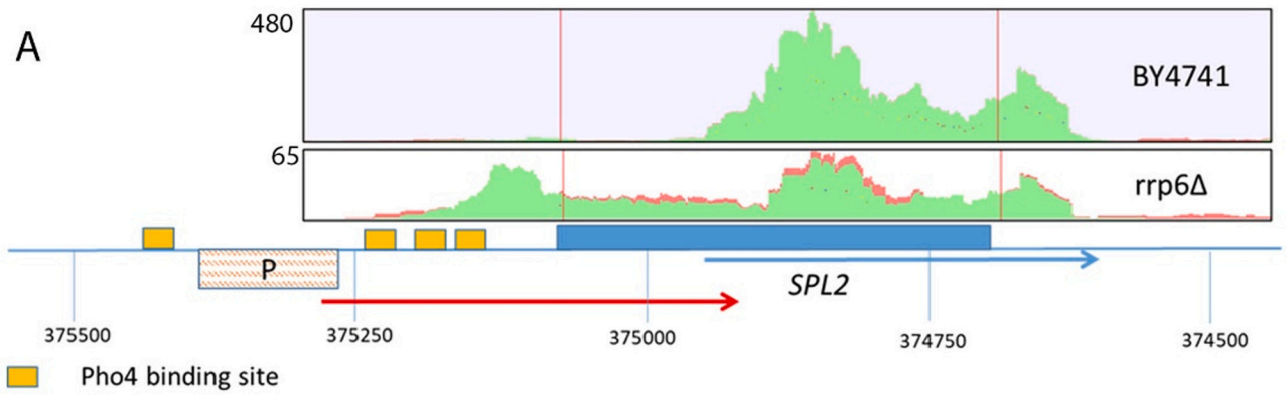

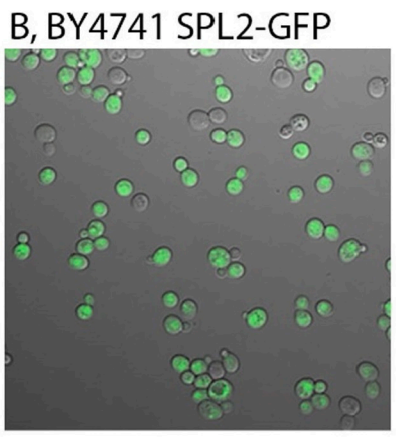

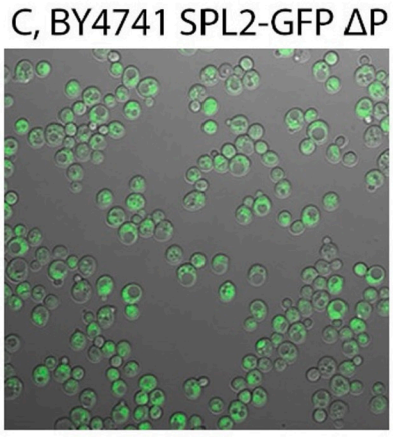

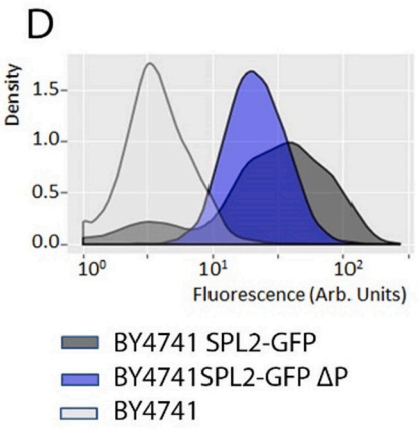

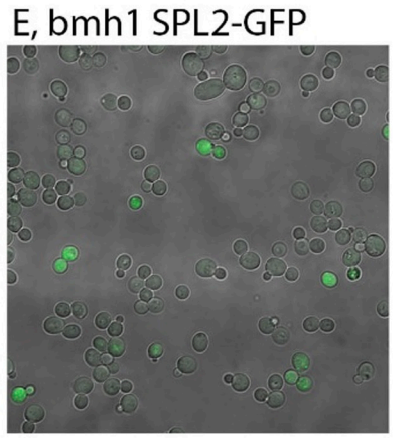

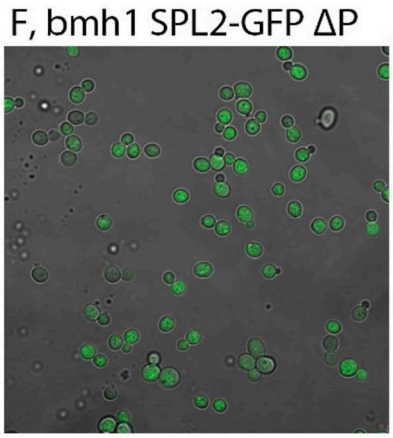

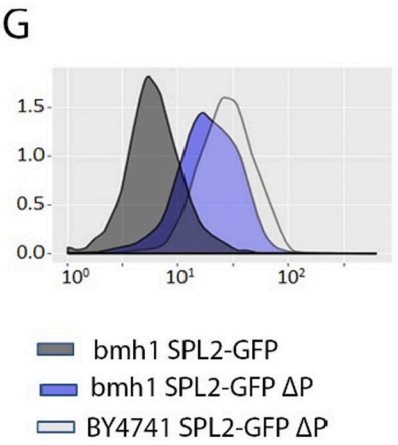

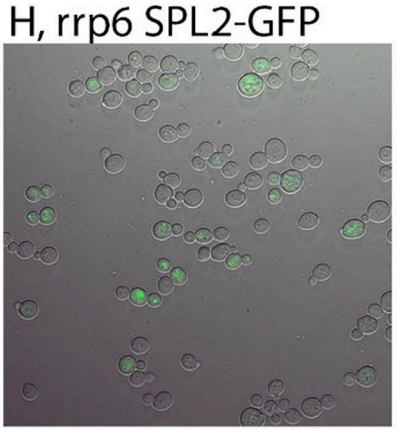

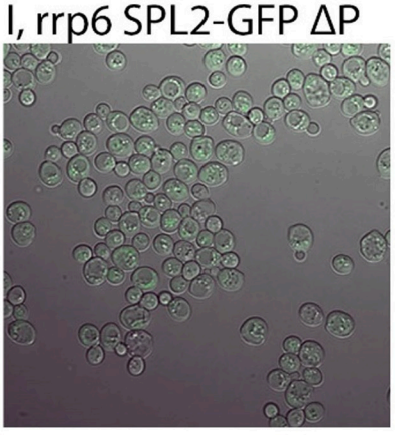

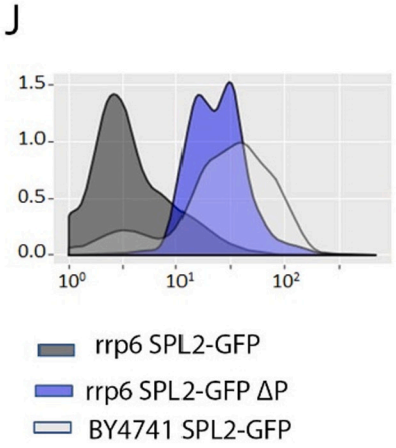

(caption on next page)

Fig. 7. Deletion of box P of the *SPL2* promoter diminishes cell-to-cell variation of *SPL2* expression. A: *SPL2* transcription. RNAseq reads of BY4741 and rrp6Δ were aligned to genomic sequences of *SPL2* using CLC Genomic Workbench (green, reads aligning in the sense direction; red, reads aligning in the antisense direction; profiles are at different scales; see also Fig. 2). The *SPL2* coding sequences are indicated with a blue box. Putative transcripts are indicated by a red and blue arrow, Pho4 binding sites by yellow boxes. Sequences deleted by the CRISPR-Cas technology are shown by the red striped box P. The numbers indicate the position at chromosome VIII as shown in SGD (www.yeastgenome.org). Confocal microscopy of BY4741 SPL2-GFP (B) of BY4741 SPL2-GFP ΔP (C), of bmh1 SPL2-GFP (E), of bmh1 SPL2-GFP ΔP (F), of rrp6 SPL2-GFP (H) and of rrp6 SPL2-GFP ΔP (I). Flow cytometry of BY4741 SPL2-GFP ΔP (D), of bmh1 SPL2-GFP ΔP (G) and of rrp6 SPL2-GFP ΔP (J) and their relevant control strains. ΔP, deletion of box P.

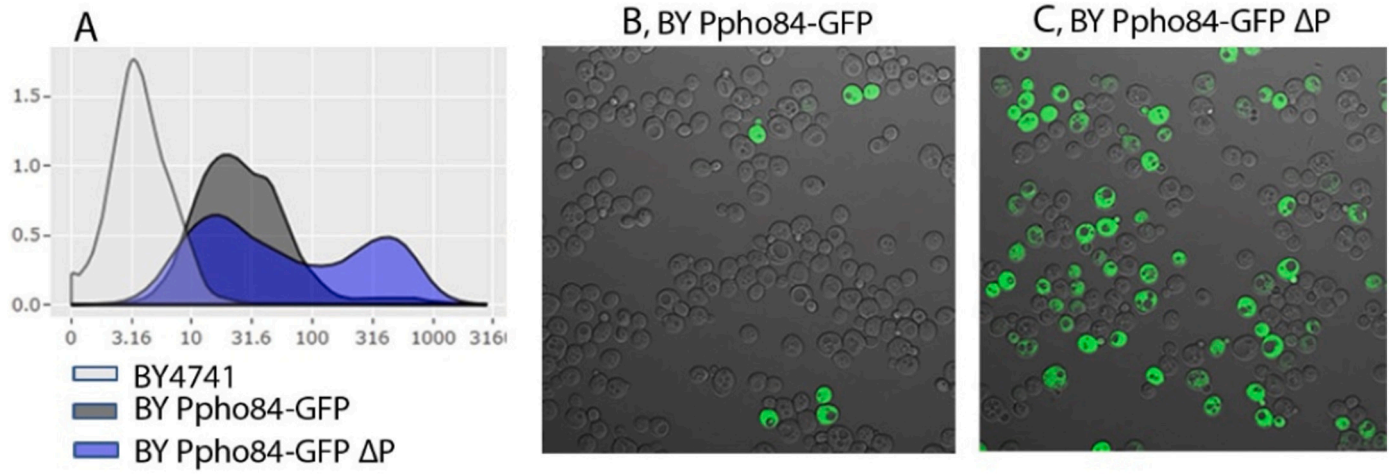

Fig. 8. Deletion of box P of the *SPL2* promoter affects the *PHO84* promoter. A: Flow cytometry of BY4741 (P_{PHO84}-GFP) ΔP, BY4741 and BY4741 (P_{PHO84}-GFP). Confocal microscopy of BY4741 (P_{PHO84}-GFP) (B) and of BY4741 (P_{PHO84}-GFP) ΔP (C). Microscopy settings used were optimal for the detection of high levels of GFP, low levels of GFP cannot be detected.

affinity phosphate transporters like Pho87 and Pho90 are mainly responsible for phosphate uptake.

In the presence of phosphate the expression of *PHO* genes is very low. However, these genes are still expressed to some extent. Expression of high affinity phosphate transporters under these conditions may be a strategy to rapidly anticipate on changes in environmental phosphate levels or may be important for phosphate sensing in line with a possible role of Pho84 in this process [46]. In our previous study [22] we showed that in the BY4741 background expression of SPL2-GFP is easily detectable in more than 90% of the cells and no expression can be found in the remaining cells. Upon phosphate starvation *SPL2-GFP* expression is strongly increased in all cells. In the bmh1Δ deletion mutant, lacking the major 14-3-3 protein isoform, RNA levels of *SPL2* and *PHO84* are strongly reduced [22] (Table 4). The effect is quite specific for these two genes as other *PHO* genes are much less affected. We further showed that in the bmh1Δ deletion mutant *SPL2-GFP* is expressed in only 20 to 30% of the cells. This observation shows that in the presence of sufficient phosphate genetically identical cells express *PHO* genes differently and that the ratio between cells expressing *SPL2* and cells not expressing *SPL2* can alter. Deletion of *RRP6*, encoding an exonuclease involved in degradation of non-coding RNA, resulted in a similar reduction in the number of cells expressing *SPL2-GFP* (Fig. 3).

Non-coding transcription (both in the sense as in the antisense direction) is involved in the regulation of the expression of many genes, both in yeast as in other organisms; for reviews see: [47–51]. It has well been established that *PHO84* expression is repressed by antisense transcription [15–17]. In this study we aligned strand-specific RNAseq reads of the bmh1Δ, spl2Δ and rrp6Δ deletion mutant to the genomic sequences of *PHO84* (Fig. 2) and found that the number of reads aligning in the sense direction was strongly reduced compared to the wild type and that the remaining reads mainly aligned to *PHO84* in the antisense direction. The number of reads of these mutants aligning in the antisense direction was comparable to the number of reads of the wild type. Using reporter constructs with GFP under control of the *PHO84* promoter we showed that this promoter is less active in the bmh1Δ, spl2Δ and rrp6Δ deletion mutants [22] (Fig. 5). Although the transcription start site of the *PHO84* antisense transcription is still unknown, alignment of RNA-seq reads suggests that antisense transcription starts just downstream of the coding region in the *PHO84* terminator. Using reporter constructs lacking this terminator we still find a reduced activity of the *PHO84* promoter in the bmh1Δ, spl2Δ and rrp6Δ deletion mutants, suggesting that antisense transcription is not causing the reduced promoter activity. This was also found in strains lacking the chromosomal *PHO84* terminator sequences indicating that *PHO84* antisense transcripts are not responsible for the reduced promoter activity by a *trans* effect (Supplementary Fig. S2).

RNAseq reads form the wild type strain BY4741 aligned to the 3′-end of the coding region of *SPL2*, whereas only few reads aligned to the 5′-end (Fig. 2A). Upon phosphate starvation many more reads aligned to *SPL2* (Fig. 2E), but not to the 5′-end. The coding region of *SPL2* may be different from the annotated coding region. Very close to the annotated start codon ATG is an upstream out of frame ATG, making it less likely that the annotated start codon is the correct start codon as mentioned before [21] (Supplementary Fig. S1A). Thus, *SPL2* translation may start at one of the downstream ATG codons. As shown in Supplementary Fig. S1 a very low GFP expression was measured using a promoter construct corresponding to the annotated start codon, whereas a much higher expression was observed using a promoter corresponding to the second downstream ATG. However, still some expression was observed using the former promoter, although at a very low level, in line with the observed use of alternative transcription start sites [37,52]. Thus, multiple different *SPL2* transcripts are present. This is further supported by the detection of peptides corresponding to the N-terminal end of the annotated Spl2 protein [53]. In an attempt to further characterize the *SPL2* transcripts we performed Northern blot analyses. Using a probe corresponding to 3′-end of *SPL2* (Fig. 1, probe B) clear bands were visible. Using a probe hybridizing to the 5′-end, only very weak bands were found (Fig. 1, probe A). Thus, the nature of the upstream transcripts still have to be disclosed.

Interestingly a few RNAseq reads did align to the 5′-end of the *SPL2*

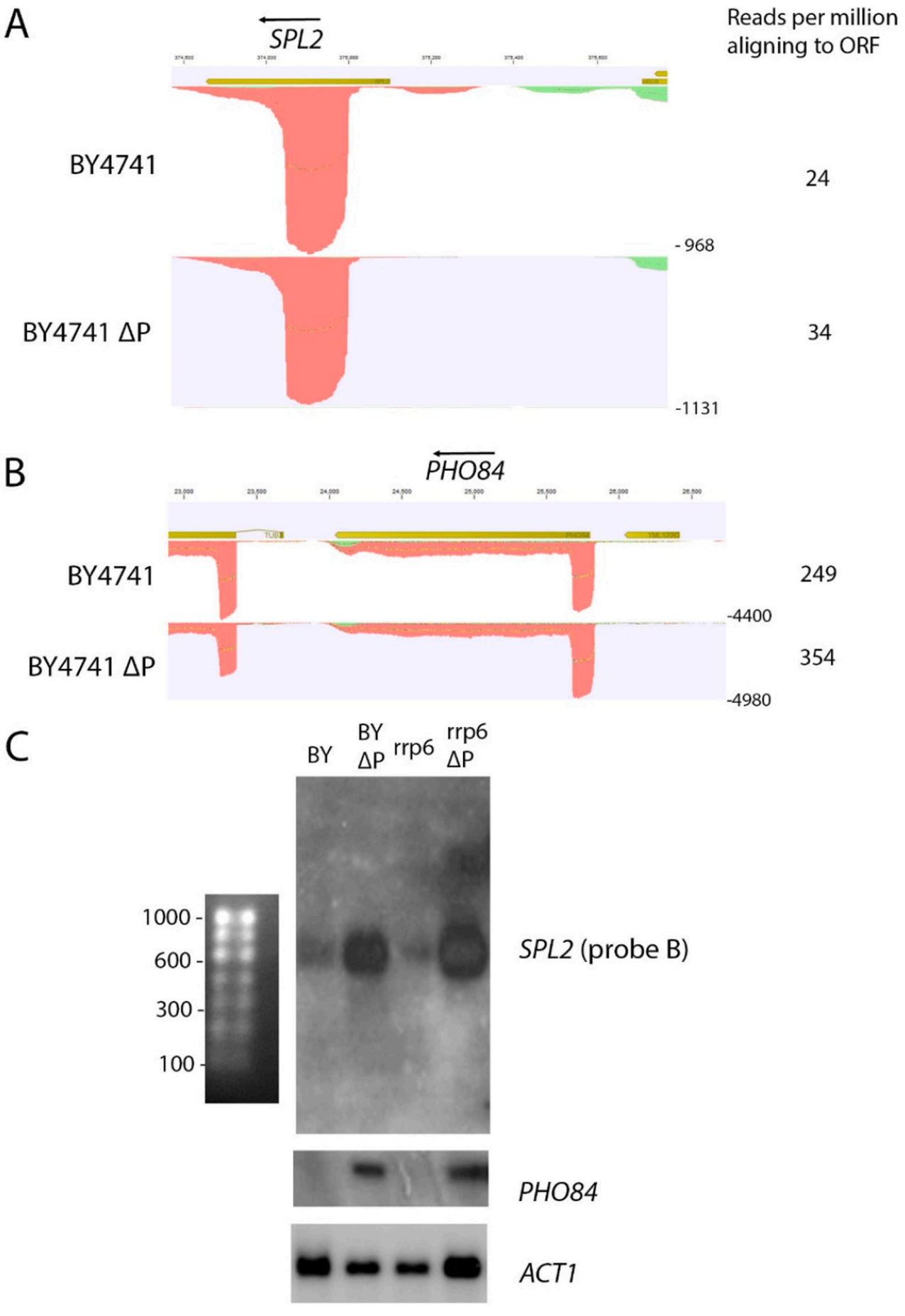

(caption on next page)

Fig. 9. Effect of deletion of box P of the *SPL2* promoter on the transcription of *SPL2* and *PHO84*. Alignment of strand-specific RNAseq reads to genomic sequences of *SPL2* (A) or *PHO84* (B). Genomic sequences (S288c) were taken from SGD (www.yeastgenome.org). Reads were aligned and alignments were visualized using CLC Genomic Workbench. Reads corresponding to the Watson-strand (left to right) are indicated in green, reads corresponding to the Crick strand (right to left) are indicated in red. Both *PHO84* and *SPL2* coding regions are located on the Crick strand. The number of reads aligning to the *SPL2* and *PHO84* open reading frames are shown (in reads per million). Northern blot analysis (C) of RNA isolated from exponentially growing cultures (A_{620} of 0.5) in YNB with 7.2 mM potassium phosphate of BY4741 (BY), BY4741 ΔP (BY ΔP), rrp6Δ and rrp6Δ ΔP. Probes were made by PCR, followed by labeling with [α-^{32}P]dCTP as described in Fig. 1. PCR Primers for the *PHO84* probe: PHO84-NB-Fw and PHO84-NB-Rev. RNA markers (RiboRuler Low Range RNA Ladder, Thermo Scientific) were visualized with ethidium bromide after blotting.

ORF or more upstream sequences and the number of these reads is relatively high in the bmh1Δ and rrp6Δ mutants. These observations suggest different transcription start sites. Data obtained by paired-end ditag sequencing of yeast RNA [52] also give evidence for upstream transcription; for visualization at SGD see: https://browse.yeastgenome.org/?loc=chrVIII%3A373197..376556&tracks=DNA%2CAll%20Annotated%20Sequence%20Features%2CDoube_strand_break_hotspots%2CXrn1-sensitive_unstable%20transcripts_XUTs%2CScGlycerolMedia%2C3%27UTRs%2CPolII_occupancy_WT%2Cantisense_internal_CUTs_SUTs_XUTs%2Cnovel_transcripts%2Cupstream_ORF&highlight=.

To address the role of this upstream transcription we deleted a part (box P) of the *SPL2* promoter in BY4741, bmh1Δ and rrp6Δ expressing *SPL2-GFP* (Fig. 7). The consequence of deletion of box P is that in BY4741 and the bmh1Δ and rrp6Δ strains almost all cells express *SPL2-GFP* in contrast to the parental strains bmh1Δ and rrp6Δ in which the majority of the cells do no express *SPL2-GFP*. RNAseq experiments showed the absence of the upstream *SPL2* transcript upon deletion of box P in BY4741 (Fig. 9). These results indicate that upstream *SPL2* transcription is determining the cell-to-cell variation of *SPL2* expression. RNAseq analysis showed that upon deletion of box P the level of RNA transcribed from the *SPL2* coding region is only modestly increased in BY4741 (Fig. 9). On the other hand Northern blot analysis showed that deletion of box P resulted in higher levels of RNA hybridizing to the *SPL2* and *PHO84* probes in both BY4741 and rrp6Δ strains (Fig. 9C), in line

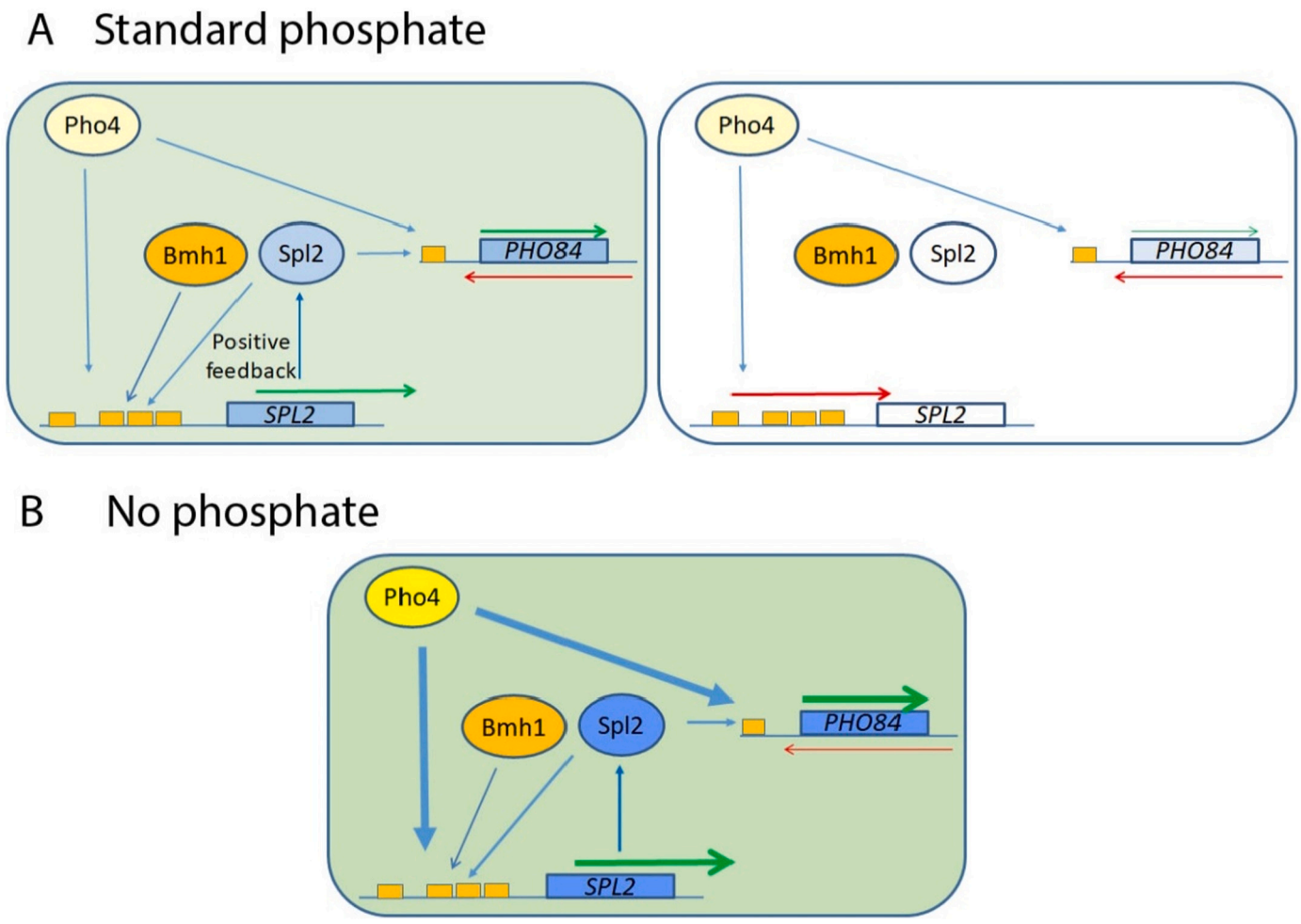

Fig. 10. Model of the regulation of *PHO84* and *SPL2* by Pho4, 14-3-3 proteins, Spl2 and non-coding transcription. A. In the presence of phosphate Pho4 is partly activated and is required for basal expression of *PHO84*. In addition, *PHO84* is transcribed in the antisense direction, although at a low level. Under these conditions either basal coding *SPL2* transcription (left panel) or upstream non-coding *SPL2* transcription (right panel) is activated. If *SPL2* coding transcription is active, the Spl2 protein stimulates its own transcription and that of *PHO84* ensuing a positive feedback (left panel). This feedback results in the bimodal *SPL2* expression and the absence of cells with intermediate *SPL2* expression. The 14-3-3 protein Bmh1 has a positive effect on *SPL2* coding transcription. B. In the absence of phosphate Pho4 is fully active and greatly stimulates both *PHO84* and *SPL2* transcription, overruling the effect of Spl2 and Bmh1. *PHO84* antisense transcription is reduced. Coding transcription is shown by green arrows, non-coding transcription by red arrows. Active genes/proteins are shown by filled blocks, inactive ones by empty blocks. Putative Pho4 binding sites [44] are indicated with yellow blocks.

with the observed effect on the expression of *SPL2-GFP* (Fig. 7). These results suggest that upstream transcription is not only responsible for the on-off state of the *SPL2* expression but also affects by an unknown mechanism the level of expression in cells in which *SPL2* transcription is active. The results are in line with a model that *SPL2* transcription is initiated either at an upstream site (within box P) or at the start site of the *SPL2* coding transcript and that removal of the upstream initiation site results in expression of *SPL2* in all cells.

It has been proposed before that positive and negative feedback loops are involved in stabilization of the expression state of *PHO* genes [21,54]. In this study we showed that deletion of *SPL2* resulted in a strong reduction of *PHO84* RNA. In addition, the *PHO84* and *SPL2* promoters are less active in the spl2Δ mutants (Fig. 5) and addition of an extra copy of *SPL2* resulted in an increased expression of *SPL2-GFP* and activation of the *PHO84* promoter (Fig. 6). These observations indicate that *SPL2* activates its own transcription and that of *PHO84*, requirements for a positive feedback.

Based on our results we refined the model describing the bimodal expression of the *PHO* genes *SPL2* and *PHO84* as postulated by Wykoff et al. [21]. In contrast to the previous model the role of Pho4 in the bimodal expression of *PHO84* and *SPL2* is less prominent. In the presence of phosphate Pho4 is only partly activated and is required for basal expression of *PHO84*. Under these conditions either basal coding *SPL2* transcription (Fig. 10A, left panel) or upstream non-coding *SPL2* transcription (Fig. 10A, right panel) is activated. The nature of the upstream transcription and the resulting transcripts have still to be characterized. Pho4 is required for *SPL2* coding transcription probably by binding to one or more of the four Pho4 binding sites (5′-CACGTG-3′) in the *SPL2* promoter. If *SPL2* coding transcription is active, the Spl2 protein stimulates its own transcription and that of *PHO84* ensuing a positive feedback. This feedback may explain the heterogeneity in *PHO* gene expression and the observations that cells either express or do not express *SPL2-GFP* and hardly any cell has an intermediate expression. The 14-3-3 protein Bmh1 has a positive effect on *SPL2* coding transcription. *PHO84* is also transcribed in the antisense direction, although at a low level. In the absence of phosphate Pho4 is fully active and greatly stimulates both *PHO84* and *SPL2* transcription, overruling the effect of Spl2 and Bmh1 (Fig. 10B). *PHO84* antisense transcription is reduced. It is still unknown how the expression state of *SPL2* is established initially. Stochastic fluctuations in the chromatin structure [55,56] or in the binding of transcription factors [57] may be important. These stochastic fluctuations may enable adaptation to environmental stresses [58–60].

Supplementary data to this article can be found online at https://doi.org/10.1016/j.bbagrm.2021.194714.

CRediT authorship contribution statement

Marjolein Crooijmans: Conceptualization, Investigation, Writing - Review & editing
Tijn Delzenne: Investigation
Tim Hensen: Investigation
Mina Darehei: Investigation
Han de Winde: Writing - Review & editing
Paul van Heusden: Conceptualization, Investigation, Writing - Original draft, Supervision.

Declaration of competing interest

The authors declare that they have no known competing financial interests or personal relationships that could have appeared to influence the work reported in this paper.

Acknowledgements

We would like to thank Christiaan Henkel for his advice on analysis of RNAseq data, Johan Memelink for his advice on Northern blot analysis and Dimitra Bloska for her help with the construction of the bmh1 SPL2-GFP ΔP strain. The initial phase of this study was funded by the Netherlands Organization for Scientific Research (NWO) - Earth and Life Sciences (ALW) (SYSMO) - grant 826.09.006 and by Generade.

References

[1] S. Zaman, S.I. Lippman, X. Zhao, J.R. Broach, How Saccharomyces responds to nutrients, Annu. Rev. Genet. 42 (2008) 27–81, https://doi.org/10.1146/annurev.genet.41.110306.130206.
[2] S. Levy, M. Kafri, M. Carmi, Barkai, Science, The competitive advantage of a dual-transporter system, 2011, pp. 1408–1412.
[3] M. Conrad, J. Schothorst, H.N. Kankipati, G. Van Zeebroeck, M. Rubio-Texeira, J. M. Thevelein, Nutrient sensing and signaling in the yeast Saccharomyces cerevisiae, FEMS Microbiol. Rev. 38 (2014) 254–299, https://doi.org/10.1111/1574-6976.12065.
[4] D.D. Wykoff, E.K. O'Shea, Phosphate transport and sensing in Saccharomyces cerevisiae, Genetics. 159 (2001) 1491–1499.
[5] J.M. Mouillon, B.L. Persson, New aspects on phosphate sensing and signalling in Saccharomyces cerevisiae, FEMS Yeast Res. 6 (2006) 171–176, https://doi.org/10.1111/j.1567-1364.2006.00036.x.
[6] P.O. Ljungdahl, B. Daignan-Fornier, Regulation of amino acid, nucleotide, and phosphate metabolism in Saccharomyces cerevisiae, Genetics. 190 (2012) 885–929, https://doi.org/10.1534/genetics.111.133306.
[7] S. Austin, A. Mayer, Phosphate homeostasis – a vital metabolic equilibrium maintained through the INPHORS signaling pathway, Front. Microbiol. 11 (2020) 1–21, https://doi.org/10.3389/fmicb.2020.01367.
[8] M. Bun-ya, K. Shikata, S. Nakade, C. Yompakdee, S. Harashima, Y. Oshima, Two new genes, PHO86 and PHO87, involved in inorganic phosphate uptake in Saccharomyces cerevisiae, Curr. Genet. 29 (1996) 344–351, https://doi.org/10.1007/s002940050055.
[9] A. Kaffman, I. Herskowitz, R. Tjian, E.K. O'Shea, Phosphorylation of the transcription factor PH04 by a cyclin-CDK complex, PHO80-PH085, Science. 263 (1994) 1153–1156.
[10] A. Komeili, E.K. O'Shea, Roles of phosphorylation sites in regulating activity of the transcription factor Pho4, Science. 284 (1999) 977–980, https://doi.org/10.1126/science.284.5416.977.
[11] K. Vogel, A. Hinnen, The yeast phosphatase system, Mol. Microbiol. 4 (1990) 2013–2017.
[12] M. Bun-ya, M. Nishimura, S. Harashima, Y. Oshima, The PH084 gene of Saccharomyces cerevisiae encodes an inorganic phosphate transporter, Mol. Cell. Biol. 11 (1991) 3229–3238, https://doi.org/10.1128/MCB.11.6.3229.Updated.
[13] J.S. Flick, J. Thorner, An essential function of a phosphoinositide-specific phospholipase C is relieved by inhibition of a cyclin-dependent protein kinase in the yeast Saccharomyces cerevisiae, Genetics. 148 (1998) 33–47.
[14] R. Ghillebert, E. Swinnen, P. De Snijder, B. Smets, J. Winderickx, Differential roles for the low-affinity phosphate transporters Pho87 and Pho90 in Saccharomyces cerevisiae, Biochem. J. 434 (2011) 243–251, https://doi.org/10.1042/BJ20101118.
[15] R. Houalla, F. Devaux, A. Fatica, J. Kufel, D. Barrass, C. Torchet, D. Tollervey, Microarray detection of novel nuclear RNA substrates for the exosome, Yeast. 23 (2006) 439–454, https://doi.org/10.1002/yea.1369.
[16] J. Camblong, N. Iglesias, C. Fickentscher, G. Dieppois, F. Stutz, Antisense RNA stabilization induces transcriptional gene silencing via histone deacetylation in *S. cerevisiae*., Cell. 131 (2007) 706–17. doi:https://doi.org/10.1016/j.cell.2007.09.014.
[17] M. Castelnuovo, S. Rahman, E. Guffanti, V. Infantino, F. Stutz, D. Zenklusen, Bimodal expression of PHO84 is modulated by early termination of antisense transcription, Nat. Struct. Mol. Biol. 20 (2013) 851–858, https://doi.org/10.1038/nsmb.2598.
[18] R. Ard, P. Tong, R.C. Allshire, Long non-coding RNA-mediated transcriptional interference of a permease gene confers drug tolerance in fission yeast, Nat. Commun. 5 (2014) 5576, https://doi.org/10.1038/ncomms6576.
[19] D. Chatterjee, A.N.A.M. Sanchez, G. Yehuda, S. Stewart, S. Beate, Transcription of lncRNA prt, clustered prt RNA sites for Mmi1 binding, and RNA polymerase II CTD phospho-sites govern the repression of Pho1 gene expression under phosphate-replete conditions in fission yeast, RNA. 22 (2016) 1011–1025, https://doi.org/10.1261/rna.056515.116.
[20] A. Garg, A.M. Sanchez, S. Shuman, B. Schwer, A long noncoding (lnc)RNA governs expression of the phosphate transporter Pho84 in fission yeast and has cascading effects on the flanking prt lncRNA and pho1 genes, J. Biol. Chem. 293 (2018) 4456–4467, https://doi.org/10.1074/jbc.RA117.001352.
[21] D.D. Wykoff, A.H. Rizvi, J.M. Raser, B. Margolin, E.K. O'Shea, Positive feedback regulates switching of phosphate transporters in *S. cerevisiae*, Mol. Cell 27 (2007) 1005–1013, https://doi.org/10.1016/j.molcel.2007.07.022.
[22] J.H.M. Teunissen, M.E. Crooijmans, P.P.P. Teunisse, G.P.H. van Heusden, Lack of 14-3-3 proteins in *Saccharomyces cerevisiae* results in cell-to-cell heterogeneity in the expression of Pho4-regulated genes SPL2 and PHO84, BMC Genomics 18 (2017), https://doi.org/10.1186/s12864-017-4105-8.
[23] G.P.H. van Heusden, D.J. Griffiths, J.C. Ford, T.F. Chin-A-Woeng, P.A. Schrader, A. M. Carr, H.Y. Steensma, The 14-3-3 proteins encoded by the BMH1 and BMH2 genes are essential in the yeast Saccharomyces cerevisiae and can be replaced by a plant homologue, Eur. J. Biochem. 229 (1995) 45–53. http://www.ncbi.nlm.nih.gov/pubmed/7744048.

[24] D. Gelperin, J. Weigle, K. Nelson, P. Roseboom, K. Irie, K. Matsumoto, S. Lemmon, 14-3-3 proteins: potential roles in vesicular transport and Ras signaling in Saccharomyces cerevisiae, Proc. Natl. Acad. Sci. U. S. A. 92 (1995) 11539–11543, https://doi.org/10.1073/pnas.92.25.11539.
[25] G.P.H. van Heusden, 14-3-3 proteins: insights from genome-wide studies in yeast, Genomics. 94 (2009) 287–293, https://doi.org/10.1016/j.ygeno.2009.07.004.
[26] R.D. Gietz, R.H. Schiestl, A.R. Willems, R.A. Woods, Studies on the transformation of intact yeast cells by the LiAc/SS-DNA/PEG procedure, Yeast. 11 (1995) 355–360.
[27] C. Janke, M.M. Magiera, N. Rathfelder, C. Taxis, S. Reber, H. Maekawa, A. Moreno-Borchart, G. Doenges, E. Schwob, E. Schiebel, M. Knop, A versatile toolbox for PCR-based tagging of yeast genes: new fluorescent proteins, more markers and promoter substitution cassettes, Yeast. 21 (2004) 947–962, https://doi.org/10.1002/yea.1142.
[28] I.G. Anemaet, G.P.H. van Heusden, Transcriptional response of Saccharomyces cerevisiae to potassium starvation, BMC Genomics 15 (2014) 1040, https://doi.org/10.1186/1471-2164-15-1040.
[29] D. Parkhomchuk, T. Borodina, V. Amstislavskiy, M. Banaru, L. Hallen, S. Krobitsch, H. Lehrach, A. Soldatov, Transcriptome analysis by strand-specific sequencing of complementary DNA, Nucleic Acids Res. 37 (2009), e123, https://doi.org/10.1093/nar/gkp596.
[30] I. Milne, G. Stephen, M. Bayer, P.J.A. Cock, L. Pritchard, L. Cardle, P.D. Shawand, D. Marshall, Using tablet for visual exploration of second-generation sequencing data, Brief. Bioinform. 14 (2013) 193–202, https://doi.org/10.1093/bib/bbs012.
[31] M.D. Robinson, D.J. McCarthy, G.K. Smyth, edgeR: a Bioconductor package for differential expression analysis of digital gene expression data, Bioinformatics 26 (2009) 139–140, https://doi.org/10.1093/bioinformatics/btp616.
[32] M.E. Schmitt, T.A. Brown, B.L. Trumpower, A rapid and simple method for preparation of RNA from, Nucleic Acids Res. 18 (1990) 3091–3092.
[33] F.L.H. Menke, S. Parchmann, M.J. Mueller, J.W. Kijne, J. Memelink, Involvement of the octadecanoid pathway and protein phosphorylation in fungal elicitor-induced expression of terpenoid indole alkaloid biosynthetic genes in Catharanthus roseus, Plant Physiol. 119 (2002) 1289–1296, https://doi.org/10.1104/pp.119.4.1289.
[34] J. Schindelin, I. Arganda-Carreras, E. Frise, V. Kaynig, M. Longair, T. Pietzsch, S. Preibisch, C. Rueden, S. Saalfeld, B. Schmid, J.-Y. Tinevez, D.J. White, V. Hartenstein, K. Eliceiri, P. Tomancak, A. Cardona, Fiji: an open-source platform for biological-image analysis, Nat. Methods 9 (2012) 676–682, https://doi.org/10.1038/nmeth.2019.
[35] P. Mitchell, E. Petfalski, A. Shevchenko, M. Mann, D. Tollervey, The exosome: a conserved eukaryotic RNA processing complex containing multiple 3′→5′ exoribonucleases, Cell. 91 (1997) 457–466, https://doi.org/10.1016/S0092-8674(00)80432-8.
[36] M.J. Fox, H. Gao, W.R. Smith-Kinnaman, Y. Liu, A.L. Mosley, The exosome component Rrp6 is required for RNA polymerase II termination at specific targets of the Nrd1-Nab3 pathway, PLoS Genet. 11 (2015) 1–26, https://doi.org/10.1371/journal.pgen.1004999.
[37] J. McMillan, Z. Lu, J.S. Rodriguez, T.H. Ahn, Z. Lin, YeasTSS: an integrative web database of yeast transcription start sites, Database. 2019 (2019) 1–12, https://doi.org/10.1093/database/baz048.
[38] J. Camblong, N. Beyrouthy, E. Guffanti, G. Schlaepfer, L.M. Steinmetz, F. Stutz, Trans-acting antisense RNAs mediate transcriptional gene cosuppression in *S. cerevisiae*, Genes Dev. 23 (2009) 1534–1545, https://doi.org/10.1101/gad.522509.
[39] Y. Liu, I. Stuparevic, B. Xie, E. Becker, M.J. Law, M. Primig, The conserved histone deacetylase Rpd3 and the DNA binding regulator Ume6 repress BOI1's meiotic transcript isoform during vegetative growth in Saccharomyces cerevisiae, Mol. Microbiol. 96 (2015) 861–874, https://doi.org/10.1111/mmi.12976.
[40] M. Chia, A. Tresenrider, J. Chen, G. Spedale, V. Jorgensen, E. Ünal, F.J. van Werven, Transcription of a 5′ extended mRNA isoform directs dynamic chromatin changes and interference of a downstream promoter, Elife. 6 (2017) 1–23, https://doi.org/10.7554/elife.27420.
[41] J. Chen, A. Tresenrider, M. Chia, D.T. McSwiggen, G. Spedale, V. Jorgensen, H. Liao, F.J. van Werven, E. Ünal, Kinetochore inactivation by expression of a repressive mRNA, Elife. 6 (2017) 1–31, https://doi.org/10.7554/elife.27417.
[42] F. Moretto, N.E. Wood, G. Kelly, A. Doncic, F.J. Van Werven, A regulatory circuit of two lncRNAs and a master regulator directs cell fate in yeast, Nat. Commun. 9 (2018), https://doi.org/10.1038/s41467-018-03213-z.
[43] K. Vogel, W. Hörz, A. Hinnen, The two positively acting regulatory proteins PHO2 and PHO4 physically interact with PHO5 upstream activation regions, Mol. Cell. Biol. 9 (1989) 2050–2057, https://doi.org/10.1128/mcb.9.5.2050.
[44] K.D. MacIsaac, T. Wang, D.B. Gordon, D.K. Gifford, G.D. Stormo, E. Fraenkel, An improved map of conserved regulatory sites for Saccharomyces cerevisiae, BMC Bioinforma. 7 (2006) 1–14, https://doi.org/10.1186/1471-2105-7-113.
[45] P. Martinez, B.L. Persson, Identification, cloning and characterization of a derepressible Na+-coupled phosphate transporter in Saccharomyces cerevisiae, Mol. Gen. Genet. 258 (1998) 628–638, https://doi.org/10.1007/s004380050776.
[46] Y. Popova, P. Thayumanavan, E. Lonati, M. Agrochão, J.M. Thevelein, Transport and signaling through the phosphate-binding site of the yeast Pho84 phosphate transceptor, Proc. Natl. Acad. Sci. U. S. A. 107 (2010) 2890–2895, https://doi.org/10.1073/pnas.0906546107.
[47] R. Ard, R.C. Allshire, S. Marquardt, Emerging properties and functional consequences of noncoding transcription, Genetics. 207 (2017) 357–367, https://doi.org/10.1534/genetics.117.300095.
[48] T. Brown, F.S. Howe, S.C. Murray, M. Wouters, P. Lorenz, E. Seward, S. Rata, A. Angel, J. Mellor, Antisense transcription-dependent chromatin signature modulates sense transcript dynamics, Mol. Syst. Biol. 14 (2018) e8007. doi: doi:10.15252/msb.20178007.
[49] M.U. Kaikkonen, K. Adelman, Emerging roles of non-coding RNA transcription, Trends Biochem. Sci. 43 (2018) 654–667, https://doi.org/10.1016/j.tibs.2018.06.002.
[50] A. Nevers, A. Doyen, C. Malabat, B. Néron, T. Kergrohen, A. Jacquier, G. Badis, Antisense transcriptional interference mediates condition-specific gene repression in budding yeast, Nucleic Acids Res. 46 (2018) 6009–6025, https://doi.org/10.1093/nar/gky342.
[51] P. Till, R.L. Mach, A.R. Mach-Aigner, A current view on long noncoding RNAs in yeast and filamentous fungi, Appl. Microbiol. Biotechnol. 102 (2018) 7319–7331, https://doi.org/10.1007/s00253-018-9187-y.
[52] Y.N. Kang, D.P. Lai, H.S. Ooi, T. Ting Shen, Y. Kou, J. Tian, D.M. Czajkowsky, Z. Shao, X. Zhao, Genome-wide profiling of untranslated regions by paired-end ditag sequencing reveals unexpected transcriptome complexity in yeast, Mol. Gen. Genomics. 290 (2014) 217–224, https://doi.org/10.1007/s00438-014-0913-6.
[53] Y. Gao, L. Ping, D. Duong, C. Zhang, E.B. Dammer, Y. Li, P. Chen, L. Chang, H. Gao, J. Wu, P. Xu, Mass-spectrometry-based near-complete draft of the Saccharomyces cerevisiae proteome, J. Proteome Res. (2021) 1328–1340, https://doi.org/10.1021/acs.jproteome.0c00721.
[54] N. Vardi, S. Levy, M. Assaf, M. Carmi, N. Barkai, Budding yeast escape commitment to the phosphate starvation program using gene expression noise, Curr. Biol. 23 (2013) 2051–2057, https://doi.org/10.1016/j.cub.2013.08.043.
[55] X. Zhou, E.K. O'Shea, Integrated approaches reveal determinants of genome-wide binding and function of the transcription factor Pho4, Mol. Cell 42 (2011) 826–836, https://doi.org/10.1016/j.molcel.2011.05.025.
[56] C.R. Brown, C. Mao, E. Falkovskaia, M.S. Jurica, H. Boeger, Linking stochastic fluctuations in chromatin structure and gene expression, PLoS Biol. 11 (2013), https://doi.org/10.1371/journal.pbio.1001621.
[57] E. Azpeitia, A. Wagner, Short residence times of DNA-bound transcription factors can reduce gene expression noise and increase the transmission of information in a gene regulation system, Front. Mol. Biosci. 7 (2020) 1–10, https://doi.org/10.3389/fmolb.2020.00067.
[58] J.M. Raser, E.K. O'Shea, Control of Stochasticity in eukaryotic gene expression, Science. 304 (2006) 1811–1814.
[59] A. Raj, A. van Oudenaarden, Nature, nurture, or chance: stochastic gene expression and its consequences, Cell. 135 (2008) 216–226, https://doi.org/10.1016/j.cell.2008.09.050.
[60] P.L. Freddolino, J. Yang, A. Momen-Roknabadi, S. Tavazoie, Stochastic tuning of gene expression enables cellular adaptation in the absence of pre-existing regulatory circuitry, Elife. 7 (2018) 1–34, https://doi.org/10.7554/eLife.31867.
[61] R.S. Sikorski, P. Hieter, A system of shuttle vectors and yeast host strains designed for efficient manipulation of DNA in Saccharomyces cerevisiae, Genetics. 122 (1989) 19–27 (doi:0378111995000377 [pii]).
[62] R.D. Gietz, A. Sugino, New yeast-Escherichia coli shuttle vectors constructed with in vitro mutagenized yeast genes lacking six-base pair restriction sites, Gene 74 (1988) 527–534. http://www.ncbi.nlm.nih.gov/pubmed/3073106.
[63] G.P.H. van Heusden, T.J. Wenzel, E.L. Lagendijk, H.Y. de Steensma, J.A. van den Berg, Characterization of the yeast BMH1 gene encoding a putative protein homologous to mammalian protein kinase II activators and protein kinase C inhibitors, FEBS Lett. 302 (1992) 145–150. http://www.ncbi.nlm.nih.gov/pubmed/1378790.
[64] M. Laughery, T. Hunter, A. Brown, J. Hoopes, T. Ostbye, T. Shumaker, J.J. Wyrick, New vectors for simple and streamlined CRISPR–Cas9 genome editing in Saccharomyces cerevisiae, Yeast. 32 (2015) 711–720, https://doi.org/10.1002/yea.